

# Hybrid Intelligent Predictive Maintenance Model for Multiclass Fault Classification

Albert Buabeng (✉ [abuabeng@umat.edu.gh](mailto:abuabeng@umat.edu.gh))

University of Mines and Technology Faculty of Engineering <https://orcid.org/0000-0001-5680-5615>

Anthony Simons

University of Mines and Technology Faculty of Engineering

Nana Kena Frimpong

Kwame Nkrumah University of Science and Technology College of Science

Yao Yevenyo Ziggah

University of Mines and Technology Faculty of Mineral Resources Technology

---

## Research Article

**Keywords:** Condition monitoring, Machine learning, Signal decomposition, Dimensionality reduction, Fault classification

**Posted Date:** July 6th, 2021

**DOI:** <https://doi.org/10.21203/rs.3.rs-600110/v1>

**License:** © ⓘ This work is licensed under a Creative Commons Attribution 4.0 International License.

[Read Full License](#)

---



22 **Abstract**

23 Data recorded from monitoring the health condition of industrial equipment are often high-dimensional,  
24 nonlinear, nonstationary and characterised by high levels of uncertainty. These factors limit the efficiency of  
25 machine learning techniques to produce desirable results when developing effective fault classification  
26 frameworks. This paper sought to propose a hybrid artificial intelligent predictive maintenance model based  
27 on Improved Complete Ensemble Empirical Mode Decomposition with Adaptive Noise (ICEEMDAN),  
28 Principal Component Analysis (PCA) and Least Squares Support Vector Machine (LSSVM) optimised by  
29 the combination of Coupled Simulated Annealing and Nelder-Mead Simplex optimisation algorithms  
30 (ICEEMDAN-PCA-LSSVM). Here, ICEEMDAN was first employed as a denoising technique to decompose  
31 signals into series of Intrinsic Mode Functions (IMFs) of which only relevant IMFs containing the relevant  
32 fault features were retained for signal reconstruction. PCA was then employed as a dimension reduction  
33 technique through which the resulting set of uncorrelated features extracted served as input for LSSVM for  
34 classifying various fault types. The proposed technique is compared with three established methods (Linear  
35 Discriminant Analysis (LDA), Support Vector Machine (SVM) and Artificial Neural Network (ANN)) with  
36 multiclass classification capabilities. The various techniques were tested on an experimental UCI machine  
37 learning benchmark data obtained from multi-sensors of a hydraulic test rig. The results from the analysis  
38 revealed that the proposed ICEEMDAN-PCA-LSSVM technique is versatile and outperformed all the  
39 compared classifiers in terms of accuracy, error rate and other evaluation metrics considered. The proposed  
40 hybrid technique drastically reduced the redundancies and the dimension of features, allowing for the efficient  
41 consideration of relevant features for the enhancement of classification accuracy and convergence speed.

42 **Keywords:** Condition monitoring, Machine learning, Signal decomposition, Dimensionality reduction, Fault  
43 classification

## 1 Introduction

As modern industrial companies strive to meet their operational targets in order to remain successful in profit maximisation, they are pressured to make use of various integrated and complex engineering machinery. Generally, working under extreme and challenging conditions, these industrial equipment are subjected to progressive deterioration, leading to a significant increase in the possibility of related component failure (Helwig et al. 2015a; Egusquiza et al. 2018). This impacts their availability and reliability to minimise operational downtime and maintenance related cost (Sheng et al. 2011). Due to these reasons, monitoring the conditions of these complicated systems as a requirement for predictive-based maintenance has gained increasing importance over the years since it determines the required maintenance action based on equipment's health status. This ensures the availability and reliability of industrial equipment and offers a significant improvement in their health condition, thus, ultimately increasing asset utilisation and reducing maintenance cost.

However, with the rising demands and increasing complexity of industrial systems, the number of installed sensors and their sampling rate are constantly growing (Schneider et al. 2018). As a result, the processing of high-dimensional data (signals) from multiple sensors for predictive-based maintenance is at risk of suffering from scalability, classification performance and the curse of dimensionality (Houle et al. 2010; Keogh and Mueen 2011; Har-Peled et al. 2012; Herrmann et al. 2012; Bach 2017). The complexity is further increased with the frequent operation of these machine components in extreme and dynamic environments, where their mode of operation is often nonlinear due to the effects of varying environmental and operating conditions such as pressure, volume flow, temperature, drift, noise and engineering variance. This contributes to the deterioration process of industrial machines or related components (Javed 2014; Helwig et al. 2015b). Consequently, the data recorded from monitoring the condition of such industrial systems are often nonlinear, nonstationary and masked with noise as output signals which are characterised by high levels of uncertainty and unpredictability (Wen 2011; Randall and Antoni 2011). Hence, the recorded data present integration and tractability challenges when developing an effective predictive framework. Therefore, there is a need to develop a robust and reliable predictive maintenance model that can tolerate uncertainty and efficiency during diverse operational conditions (Zhang and Randall 2009; Sarkar 2015; Wang 2017).

In literature, Machine Learning (ML) algorithms are among the most powerful and frequently used techniques in developing intelligent predictive maintenance frameworks in various applications (Çınar et al. 2020a). This is due to the enormous potential of ML algorithms to process multivariate and high-dimensional dataset (generated in industries by industrial equipment and machinery) through the extraction of hidden patterns, classification, prediction or visual representation (Helwig et al. 2015a; Raptodimos and Lazakis 2018; Kaur and Kaur 2020). However, a sizable number of these ML algorithms are very task-specific and thus are incapable of being implemented in other specialised tasks. Hence, their performance varies when implemented independently. Also, these ML algorithms are further constrained in producing the desired results when exposed to nonlinear and nonstationary high-dimensional datasets characterised by high levels of uncertainties (Cho et al. 2018). For these reasons, researchers in the field of predictive maintenance have directed their focus into building hybrid frameworks by leveraging on the strength and weakness of the multiple ML algorithms which unquestionably are improvements of existing techniques (Zhang et al. 2014; Chakraborty 2017; Di et al. 2019). Thus, a hybrid approach for analysing high-dimensional data has gained significant attention in the development of predictive maintenance frameworks, but little has been reported in literature. Hence, this study proposes a hybrid synergistic framework for classifying fault conditions based on the Improved Complete Ensemble Empirical Mode Decomposition with Adaptive Noise (ICEEMDAN), Principal Component Analysis (PCA) and the Least Squares Support Vector Machine (LSSVM) optimised by Coupled Simulated Annealing (CSA) and Nelder-Mead Simplex (NMS) optimisation algorithms.

The motivation for creating the hybrid is that, for ICEEMDAN, it has the ability to decompose nonlinear and nonstationary signals arising from complex systems into a series of Intrinsic Mode Functions (IMFs), where each resulting IMF represents the respective local transient features (Colominas et al. 2014). Besides, when compared to existing filtering techniques for extracting transient features from nonlinear and nonstationary signals such as the Wigner-Ville Distribution (WVD) (Wigner 1932), Short-Time Fourier Transform (STFT) (Peppin 1994; Newland 2005), Wavelet Transform (WT) (Daubechies 1989) and Empirical Mode

95 Decomposition (EMD) (Huang et al. 1998), the ICEEMDAN drastically reduces the contamination of noise  
96 in a signal and the issue of mode mixing. In so doing, the inability to separate different frequencies into  
97 separate IMF's has been greatly resolved. However, despite the good performance of ICEEMDAN, not much  
98 attention has been given regarding its application in the field of engineering (Zhang et al. 2018). Hence, this  
99 study introduces ICEEMDAN to denoise the signals and reduce the level of uncertainties that might have  
100 been introduced into our dataset due to the effects of varying environmental and operating conditions. In the  
101 case of PCA, it is a widely-known fact that processing of high-dimensional data which is typical of modern  
102 industries (i.e. generally, lots of measured processes, often in high and varying sampling rates are collected  
103 in order to detect and control the process) further complicates the model development phase due to numerous  
104 features. Hence, building an artificial intelligent fault classifier requires the utilisation of an efficient feature  
105 extraction and selection technique as they play a vital role in detecting relevant features in the classification  
106 space (Cho and Hoang 2017). As such, PCA is employed to extract the relevant features that contain the most  
107 characteristic fault information for each measured process. The PCA will further reduce the redundant  
108 influence and as well generate a set of linearly uncorrelated features to serve as inputs to the artificial  
109 intelligent classifier, LSSVM. The LSSVM technique was adopted as the intelligent classifier as it converts  
110 the inequality constraints from the classical SVM into linear equations for enhancing the computational  
111 capability and design over standard SVMs and Artificial Neural Networks (ANNs) (Suykens and Vandewalle  
112 1999; Suykens et al. 2002). However, the classification accuracy of LSSVM is highly influenced by the  
113 regularisation and kernel parameters. Thus, the selection of an optimal regularisation and kernel parameters  
114 play a significant role in classification performance by distributing samples in a given search space (Cho and  
115 Hoang 2017; Mosavi and Edalatifar 2018). In literature, the use of optimisation algorithms such the Particle  
116 Swarm Optimisation (PSO) (Kennedy and Eberhart 1995), Genetic Algorithm (GA) (Whitley 1994), Ant  
117 Colony Optimization (ACO) (Dorigo et al. 2006), Differential Evolution (DE) (Ilonen et al. 2003), Artificial  
118 Bee Colony (ABC) (Karaboga et al. 2014), Gravitational Search Algorithm (GSA) (Rashedi et al. 2009) and  
119 others for estimating such parameters has been greatly explored. However, considering the theory of No Free  
120 Lunch [58] which implies that no single optimiser can boast of being superior to the others for all optimisation  
121 tasks, and as such meta-heuristics are task-specific, inspires the selection of CSA-NMS hybrid optimisation  
122 algorithms as the choice for estimating the optimal parameters required for training the LSSVM classifier in  
123 this study. The hybrid CSA-NMS is a computationally fast global optimiser with high local optima avoidance  
124 capability while the NMS is utilised for fine-tuning the regularisation and kernel parameters. Hence, the  
125 CSA-NMS improves the convergence speed (i.e. considerable reduction in time complexity) and  
126 classification accuracy for fault detection.

127 In continuance of that, the contributions of this study are to:

- 128 (a) proposes a hybrid synergistic ML predictive maintenance framework of ICEEMDAN-PCA-LSSVM  
129 for fault classification capable of effectively handling high levels of uncertainty from complex,  
130 nonlinear and diverse operational conditions of machinery; and
- 131 (b) evaluate and compare the performance of the proposed hybrid approach with its variants as well as  
132 some well-established ML classifiers.

133 The efficiency of the proposed hybrid ICEEMDAN-PCA-LSSVM technique is verified by applying to the  
134 University of California, Irvine (UCI) machine learning benchmark data obtained from multi-sensors of a  
135 hydraulic system (Helwig et al. 2015a). The proposed hybrid ICEEMDAN-PCA-LSSVM technique reduces  
136 the redundancies and the dimension of features, allowing for the efficient consideration of relevant features  
137 for the enhancement of classification accuracy and convergence speed. Moreover, the proposed hybrid  
138 technique advances the field of predictive maintenance by improving the general performance of feature  
139 extraction and fault diagnosis framework for various complex and nonlinear operational environment  
140 systems.

141 The remaining sections of the paper are organised as follows. Section 2 discusses some related works in the  
142 field of predictive maintenance. Section 3 describes the complex hydraulic system UCI benchmark dataset.  
143 Section 4 introduces the proposed hybrid ICEEMDAN-PCA-LSSVM technique and briefly presents the  
144 ICEEMDAN, PCA, optimised LSSVM techniques. Section 5 describes the application of the proposed

145 technique to multiclass fault classification of the complex hydraulic system. Concluding remarks are  
146 presented in Section 6.

## 147 **2 Related works**

148 As discussed in the introductory section, ML algorithms have extensively been used in solving numerous and  
149 diverse industrial problems such as predictive maintenance of manufacturing systems, machines and related  
150 components. A recent review of articles from academic databases (Scopus, ScienceDirect, Institute of  
151 Electronic and Electrical Engineers (IEEE) and Google Scholar) conducted by Çınar et al. (2020) on the  
152 application of ML algorithms in predictive maintenance within 2010 to 2020 yielded 788 research works as  
153 at July 30, 2020. Upon further limiting the search scope to only engineering, energy and material science  
154 (excluding reviews and conference reviews) resulted in 217 research works (Çınar et al. 2020b). However,  
155 among these 217 research works, most were published from the year 2015 to 2020, suggesting that the  
156 implementation of ML algorithms in the field of predictive maintenance is a relatively new approach with  
157 growing interesting in the world of science.

158 To collect related works pertaining to this study, specific keywords such as predictive maintenance, machine  
159 learning, fault classification and hydraulic system were used to search the various academic and scholarly  
160 databases. The search period was specified from 2015 to 2021 in order to produce the ML techniques that  
161 have used in predictive maintenance with a key interest in hydraulic systems, and how they have evolved  
162 over the years. The search displayed almost 100 research works, all focusing on various engineering setups  
163 utilising hydraulic components (Gomes et al. 2016; Xu et al. 2017a; Hao et al. 2020; Pugin 2020). Aside from  
164 the general maintenance of the hydraulic system, other research works focus on specific key components such  
165 as the valve (Vianna et al. 2015; Karanović et al. 2019; Lei et al. 2019), pump (Wang et al. 2016; Xu et al.  
166 2017b; Casoli et al. 2019), accumulator (Niu et al. 2016; Pfeffer et al. 2016; Leon-Quiroga et al. 2020), cooler  
167 (Hathaway et al. 2018).

168 For a better comprehension of this study, the scope of the related works is further limited to prior works  
169 conducted using the same hydraulic system dataset (obtained from the UCI machine learning repository)  
170 employed. This will allow the tracking of progress that has been made regarding the usage of ML algorithms  
171 in monitoring the conditions of the considered hydraulic system data since its inception in 2015. Table 1  
172 summarises the ML algorithms that have been utilised in developing predictive maintenance methods based  
173 on the UCI machine learning repository hydraulic system dataset under consideration. As seen, since the  
174 publication of the considered hydraulic dataset by Helwig et al. (2015), several works that have been  
175 conducted attempt to proposed predictive maintenance techniques that improve upon the efficiency and  
176 accuracy in classifying the four major components (accumulator, cooler, pump and valve conditions).  
177 Although improvements have been realised over the years, there still exist some aspects of the dataset that is  
178 yet to be explored. Hence, this study introduces the ICEEMDAN denoising technique as the first phase of  
179 pre-processing for dealing with high levels of uncertainties introduced into the dataset as a result of the  
180 nonlinear and dynamic operational conditions of engineering systems. Comparing the prior works, it was  
181 found that none of the existing studies addressed the issue of uncertainty (noise) before classifying the  
182 degradation states of the monitored conditions. Therefore, performing data denoising as a pre-processing step  
183 is a contribution to knowledge in predictive maintenance.

## 184 **3 Condition monitoring of hydraulic system dataset**

185 Time series data recorded from monitoring the condition of a hydraulic system is obtained from the UCI ML  
186 repository via <http://archive.ics.uci.edu/ml/datasets/Condition+monitoring+of+hydraulic+systems>. The  
187 essential details of the dataset are briefly discussed in this section, with detailed discussion found at the source  
188 (Helwig et al. 2015a). The dataset comprised of raw sensor readings with different sampling rates  
189 corresponding to different number of attributes (60 – 6000) per sensor. In all, the data consisting of 17 process  
190 sensors were made up of 2205 instances and 43680 attributes. The dataset also contains fault scenarios  
191 depicting the variations in fault condition (health status) of major components such as hydraulic accumulator,  
192 cooler, internal pump leakage and valve. The details of the hydraulic system dataset are shown in Table 2.

#### 193 **4 Proposed hybrid technique (ICEEMDAN-PCA -LSSVM)**

194 Fig. 1 shows the schematic of the proposed synergistic hybrid technique from the data pre-processing stage  
195 through to the classification stage. First, ICEEMDAN is employed as a denoising technique to decompose  
196 the nonlinear and nonstationary signals into a series of IMFs of which only relevant IMFs containing the fault  
197 features are retained for the reconstruction of the signal. The selection of relevant IMFs is based on the  
198 stringent threshold for discriminating between relevant and spurious IMFs proposed by Ayenu-Prah and  
199 Attoh-Okine (2010). Statistical time-domain features that represent the shape and distribution of the signals  
200 are then extracted. PCA is then used to generate a set of uncorrelated features from which relevant features  
201 are selected to serve as input parameters for the LSSVM optimised by CSA-NMS for classifying fault types.  
202 The details of the various stages shown in Fig. 1 and the methods used are discussed in the subsequent  
203 sections.

#### 204 **4.1 Data pre-processing**

205 Most machine components are often operated in extreme and dynamic environments where its mode of  
206 operation and the data recorded from monitoring the condition of such machinery are often nonlinear,  
207 nonstationary and masked with noise as output signals which are characterised by high levels of uncertainty  
208 and unpredictability (Wen 2011; Randall and Antoni 2011). These limitations present integration and  
209 tractability challenges when developing effective classification and predictive models. Thus, in order to  
210 develop a robust and reliable predictive maintenance model from noisy signals, a reliable technique for pre-  
211 processing (denoising) and extracting relevant features is required.

212 In literature, among the frequently used techniques for pre-processing (denoising) and extracting relevant  
213 features from such signals (data sets) is to decompose the signals into transient features. Over the years,  
214 techniques such as Wigner-Ville Distribution (WVD) (Wigner 1932), Short-Time Fourier Transform (STFT)  
215 (Peppin 1994; Newland 2005), Wavelet Transform (WT) (Daubechies 1989) and Empirical Mode  
216 Decomposition (EMD) (Huang et al. 1998) have been employed for extracting transient features from  
217 nonlinear and nonstationary signals. However, studies have shown that these methods have some limitations.  
218 For example, the WVD is useful in extracting transient features in time-frequency signals but cannot account  
219 for the local transient features of the signals at a given time and presents cross-terms when signal with many  
220 frequency components is being analysed. Moreover, WVD spreads noise and may result in negative amplitude  
221 values which are irrelevant leading to further complications (Cohen 1989; Marwala 2012). As opposed to the  
222 WVD, the STFT is useful in extracting the localised transient feature by transforming a small-time window  
223 into a frequency domain. Conversely, STFT is restricted as any increase in the time resolution negatively  
224 affects the frequency resolution, and vice versa (Hlawatsch and Boudreaux-Bartels 1992). As a remedy, the  
225 WT was proposed as an efficient alternative for dealing with fixed time-frequency resolution problems and  
226 transient signals in general (Galli et al. 1996). Nonetheless, a low resolution is attained at higher frequencies  
227 as the frequency from WT is logarithmically scaled (Barschdorff and Femmer 1995).

228 To overcome the deficiencies of these techniques, a nonparametric feature extraction method, the EMD was  
229 proposed to decompose nonlinear and nonstationary signals arising from complex systems into a series of  
230 Intrinsic Mode Functions (IMFs), where each resulting IMF represents the respective local transient features  
231 (Huang et al. 1998). On the contrary, the issue of mode mixing, that is, the inability to separate different  
232 frequencies into separate IMF's is a major drawback of the EMD (Haddar 2018; Mahgoun et al. 2018; Cheng  
233 et al. 2019). To eliminate the mode mixing problem, a noise-assisted version, the Ensemble EMD (EEMD)  
234 that involves adding gaussian white noise to the original signals was proposed (Wu and Huang 2009).  
235 However, the resulting reconstructed signals led to the formation of extra modes which requires extra iteration  
236 effort to decompose the given signal. To optimise the decomposition of signals whiles reducing reconstruction  
237 error, the Complete Ensemble EMD with Adaptive Noise (CEEMDAN) (Torres et al. 2011) has been  
238 proposed. In this study, the recently enhanced formulation of CEEMDAN known as the Improved Complete  
239 Ensemble EMD with Adaptive Noise (ICEEMDAN) that has the ability to reduce the contamination of noise  
240 in a signal (Colominas et al. 2014) is adopted. ICEEMDAN is proposed as a pre-processing technique to  
241 extract the required fault features whiles reducing the noise and high levels of uncertainty.

242 **4.1.1 Improved Complete Ensemble EMD with Adaptive Noise (ICEEMDAN)**

243 The ICEEMDAN is an adaptive method for decomposing nonlinear and nonstationary signals (both time and  
 244 frequency domains) into a series of Intrinsic Mode Functions (IMFs), where each resulting IMF represents  
 245 the respective local transient features (Huang et al. 1998). The ICEEMDAN technique, has great  
 246 improvement on the Ensemble EMD (EEMD) and Complete Ensemble EMD (CEEMD) methods, as was  
 247 stated in Section 4.1. The ICEEMDAN is illustrated by the addition of a Gaussian noise series to the actual  
 248 signal as shown in Equation (1).

249 
$$x^i(t) = x(t) + \beta_0 E_1(w^i(t)) \quad (1)$$

250 where  $x(t)$  is the signal,  $\beta_{i-1} = \varepsilon_{i-1} \text{std}(x) / \text{std}(E_i(w^i(t)))$  is the ratio coefficient,  $E_k(\cdot)$  is the operator for  
 251 producing the  $k^{\text{th}}$  IMF generated by EMD,  $w^i(t)$  is a realisation of unit variance white Gaussian noise with  
 252 a zero mean.

253 Using Equation (1), EMD is used to gain the first residual ( $r_1$ ) of the signal by computing the local mean of  
 254  $I$  realisations as shown in Equation (2).

255 
$$r_1 = \langle M(x^i(t)) \rangle \quad (2)$$

256 where  $M(\cdot)$  is the operator for estimating the local mean.

257 For the first IMF,  $k = 1$ , is estimated using Equation (3).

258 
$$IMF_1 = x(t) - r_1 \quad (3)$$

259 The second residual ( $r_2$ ) is estimated as the average of the local means of the realisations as shown in  
 260 Equation (4).

261 
$$r_2 = \langle M(r_1 + \beta_1 E_2(w^i(t))) \rangle \quad (4)$$

262 Then, the second IMF at  $k = 2$  is estimated using Equation (5).

263 
$$IMF_2 = r_1 - r_2 \quad (5)$$

264 The  $k^{\text{th}}$  residual and  $k^{\text{th}}$  IMF are estimated using Equations (6) and (7), respectively.

265 
$$r_k = \langle M(r_{k-1} + \beta_{k-1} E_k(w^i(t))) \rangle \quad (6)$$

266 
$$IMF_k = r_{k-1} - r_k \quad (7)$$

267 The process from Equations (6) and (7) is repeated for the next  $k$ .

268 **4.1.2 Signal reconstruction**

269 In the application of the ICEEMDAN on the data, it is of paramount importance to select the relevant IMFs  
 270 which contains as much fault information as possible from the series of IMFs generated by ICEEMDAN  
 271 while neglecting the spurious IMFs. As such, an effective, quick and repeatable scientific framework is  
 272 needed to discriminate between relevant and spurious IMFs for the signal reconstruction to aid improve the  
 273 performance of the fault diagnosis system. In this paper, a stringent threshold for discriminating between  
 274 relevant and spurious IMFs in the presence of high levels of noise, proposed by Ayenu-Prah and Attoh-Okine  
 275 (2010) is employed as the criterion for selecting the relevant IMFs. The stringent threshold ( $\lambda$ ) is expressed  
 276 as a function of the correlation coefficient ( $\rho$ ) between the observed signal  $x(t)$ , and each  $IMF_i$ , as shown  
 277 in Equation (8).

278 
$$\lambda = \frac{\max(\rho_i)}{10 \times \max(\rho_i) - 3}, \quad i = 1, 2, K, k \quad (8)$$

279 where  $\rho_i$  is estimated using Equation (9).

280 
$$\rho_i = \frac{\text{cov}(x(t), IMF_i)}{\sqrt{\text{cov}(x(t), x(t)) \bullet \text{cov}(IMF_i, IMF_i)}} \quad (9)$$

281 Using Equation (8), an IMF is regarded as relevant if its corresponding  $\rho_i \geq \lambda$ . After identifying all the  
282 relevant IMFs, they are then summed to form the reconstructed signal for subsequent analysis.

283 It must be noted that the standard ICEEMDAN algorithm proposed by Colominas et al. (2014) whose source  
284 code is found at [http://bioingenieria.edu.ar/grupos/ldnllys/meteorres/re\\_inter.htm#Codigos](http://bioingenieria.edu.ar/grupos/ldnllys/meteorres/re_inter.htm#Codigos), allows for the  
285 decomposition of only one signal or feature or univariate series into IMF's at a time. Hence, the  
286 implementation of ICEEMDAN using the above source code becomes practically impossible with high-  
287 dimensional datasets which is the domain of this study. To overcome this drawback, the standard  
288 ICEEMDAN algorithm is modified by integrating the stringent threshold (Equation (8)) as a criterion for  
289 discriminating between relevant and spurious IMFs, and finally converting to an iterative algorithm using the  
290 *for loop* function such that the decomposition followed reconstruction will be done for all features. This  
291 modification extended the capabilities of the standard ICEEMDAN source code by automating the  
292 decomposition and reconstruction of multiple signals all in a single execution of the algorithm as shown in  
293 Fig. 2.

## 294 4.2 Feature extraction and selection

295 After denoising the 17 process sensors using the ICEEMDAN technique discussed in the previous section,  
296 the next issue that needs to be addressed is the dimension of features (43680), which is relatively high.  
297 Consequently, conventional ML techniques will suffer from tractability, scalability, high time complexities  
298 and more importantly classification performance issues (Houle et al. 2010; Keogh and Mueen 2011; Har-  
299 Peled et al. 2012; Herrmann et al. 2012; Bach 2017). Also, feeding the denoised dataset directly into  
300 conventional ML techniques fails to detect features that contain the most characteristic fault information  
301 required for the efficient classification of the fault conditions (Chawathe 2019). Hence, a well-established  
302 strategy is to extract some statistics-based features or transforms that represents the characteristic properties  
303 of the hydraulic dataset from the 43680 denoised features.

### 304 4.2.1 Extraction of statistical features

305 In prior works such as Helwig et al. (2015a, b), the hydraulic system dataset was partitioned into various time  
306 intervals. In this study, as a means of ensuring uniformity within all cycles, the various time intervals were  
307 allocated after averaging each feature per sensor. Also, similar to prior research works where the data for each  
308 cycle per sensor were all partitioned into various segments, the partitioning of the cycles in this study varied  
309 with varying characteristic time intervals of the cycles. Fig. 3(a), for instance, shows 13 characteristic time  
310 intervals after averaging each feature in the PS1 sensor data. Similarly, PS5 was partitioned into 19  
311 characteristic time intervals as shown in Fig. 3(b). The column labelled "Time Interval" in Table 2 shows the  
312 various number of characteristic time intervals each sensor was segmented into. Different statistical time-  
313 domain features such as mean, median, variance, standard deviation, skewness, kurtosis and maximum peak  
314 value in each segment were then extracted. This resulted in a pool of 1806 features (approximately 2418.61%  
315 reduction). However, building an intelligent classifier with all the 1806 features which is still high in terms  
316 of dimension will significantly increase the complexity of the framework. Therefore, before an artificial  
317 intelligent fault classifier can be applied to the resulting pool of 1806 features, it is imperative for a second  
318 stage involving dimensionality reduction to be carried out. Hence, this study employs the PCA, an effective  
319 dimensionality reduction technique. The PCA is capable of extracting relevant features containing the most  
320 characteristic fault information from the resulting pool of 1806 time-domain features extracted from the  
321 reconstructed signals.

### 322 4.2.2 Principal Component Analysis (PCA)

323 PCA is one of the standard unsupervised techniques often used to effectively transform large sets of features  
324 into few independent and uncorrelated features while retaining as maximum variability as possible. The  
325 algorithm is summarised as follows.

326 Suppose  $X = (X_1, X_2, \dots, X_p)^T$  is a random vector of features of  $p$  dimension with population covariance  
327 matrix as shown in Equation (10).

328

$$\Sigma_X = \begin{pmatrix} \sigma_1^2 & \sigma_{12} & L & \sigma_{1p} \\ \sigma_{21} & \sigma_2^2 & L & \sigma_{2p} \\ M & M & O & M \\ \sigma_{p1} & \sigma_{p2} & L & \sigma_p^2 \end{pmatrix} \quad (10)$$

329 Consider the linear combination expressed in Equation (11).

330

$$\begin{aligned} Y_1 &= e_{11}X_1 + e_{12}X_2 + L + e_{1p}X_p \\ Y_2 &= e_{21}X_1 + e_{22}X_2 + L + e_{2p}X_p \\ M & \quad M \quad M \quad M \quad M \\ Y_p &= e_{p1}X_1 + e_{p2}X_2 + L + e_{pp}X_p \end{aligned} \quad (11)$$

331 Each linear combination in Equation (11) can be thought of as linear regression, predicting  $Y_i$  using  
332  $X_1, X_2, K, X_p$  where  $e_{i1}, e_{i2}, K, e_{ip}$  are the regression coefficients.

333  $Y_1$ , the first Principal Components (PC1) is the linear combination of  $X_i$  such that,  $Y_1$  accounts for the  
334 maximum variation in the data as shown in Equation (12).

335

$$\text{var}(Y_1) = \sum_{k=1}^p \sum_{l=1}^p e_{1k} e_{1l} \sigma_{kl} \quad (12)$$

336 As such,  $e_{11}, e_{12}, K, e_{1p}$  are defined such that maximum variance is achieved, subject to the constraint shown  
337 in Equation (13).

338

$$\sum_{j=1}^p e_{1j}^2 = 1 \quad (13)$$

339  $Y_2$ , the second Principal Component (PC2) is the linear combination  $X_i$  such that,  $Y_2$  accounts for as much  
340 variance remaining after PC1, as shown in Equation (14).

341

$$\text{var}(Y_2) = \sum_{k=1}^p \sum_{l=1}^p e_{2k} e_{2l} \sigma_{kl} \quad (14)$$

342 As such,  $e_{21}, e_{22}, K, e_{2p}$  are selected to maximise the variance of  $Y_2$ , subject to the constraint shown in  
343 Equation (15).

344

$$\sum_{j=1}^p e_{2j}^2 = 1 \quad (15)$$

345 For  $Y_i$ , the  $i^{\text{th}}$  Principal Component,  $(e_{i1}, e_{i2}, K, e_{ip})$  selected to maximise the variance of  $Y_i$  (Equation  
346 (16), subject to the constraint shown in Equation (17).

347

$$\text{var}(Y_i) = \sum_{k=1}^p \sum_{l=1}^p e_{ik} e_{il} \sigma_{kl} \quad (16)$$

348

$$\sum_{j=1}^p e_{ij}^2 = 1 \quad (17)$$

349 All PC's generated are uncorrelated, that is,  $\text{cov}(Y_{i-1}, Y_i) = 0$  and will serve as the inputs data for the artificial  
350 intelligent classifier.

351 **4.3 Classification and parameter optimisation**

352 **4.3.1 Least Squares Support Vector Machine (LSSVM)**

353 The LSSVM technique as proposed by Suykens and Vandewalle (Suykens and Vandewalle 1999) is an  
 354 extended least squares version of the standard SVM classifier. LSSVM imposes equality constraints by  
 355 utilising a set of linear equations formulated from all training data during the training process. Thus,  
 356 enhancing LSSVMs computational capability and generalisation over standard SVMs whiles reducing  
 357 computational complexity.

358 Suppose  $\{x_i, y_i\}$  is a random vector of training features, for  $i=1,2,K,n$  instances, where input features with  
 359 its corresponding target are  $x_i \in \mathbb{R}^n$  and  $y_i \in \mathbb{R}$ , respectively. The LSSVM formulated is expressed as an  
 360 optimisation problem with the objective function shown in Equation (18) subject to the equality constraint  
 361 shown in Equation (19).

362 
$$\min_{\omega, b, \xi} J(\omega, b, \xi) = \frac{1}{2} \omega^T \omega + \gamma \frac{1}{2} \sum_{i=1}^n \xi_i^2 \quad (18)$$

363 
$$y_i = \omega^T \phi(x_i) + b + \xi_i^2, \quad i = 1, 2, K, n \quad (19)$$

364 where  $J(\omega, b, \xi)$  is the objective function with weight vector dimensional space  $\omega \in \mathbb{R}^n$ , error variables  
 365  $\xi_i \in \mathbb{R}$  and bias term  $b$ .  $\gamma$  is an influential positive penalty factor of the trade-off between the margin and  
 366 training error,  $\phi(\cdot)$  is a function which maps the input space into a high-dimensional space.

367 The LSSVM model is expressed as shown in Equation (20).

368 
$$f(x) = \omega^T \phi(x) + b \quad (20)$$

369 Using Equation (18), a Lagrangian  $L$ , is then defined (Equation (21)).

370 
$$L(\omega, b, \xi; \alpha) = J(\omega, b, \xi) - \sum_{i=1}^n \alpha_i (\xi_i - y_i + \omega^T \phi(x_i) + b) \quad (21)$$

371 where  $\alpha_i \in \mathbb{R}$  is the Langrage multiplier, which follows the Karush-Kuhn-Tucker optimality conditions as  
 372 shown in Equation (22).

373 
$$\begin{cases} \frac{\partial L}{\partial \omega} = 0 \rightarrow \omega = \sum_{i=1}^n \alpha_i \phi(x_i) \\ \frac{\partial L}{\partial b} = 0 \rightarrow \sum_{i=1}^n \alpha_i = 0 \\ \frac{\partial L}{\partial \xi_i} = 0 \rightarrow \alpha_i = \gamma \xi_i \\ \frac{\partial L}{\partial \alpha_i} = 0 \rightarrow \xi_i - y_i + \omega^T \phi(x_i) + b = 0 \end{cases} \quad (22)$$

374 A solution (Equation (23)) is obtained after eliminating  $\omega$  and  $\xi_i$ .

375 
$$\begin{bmatrix} 0 & 1_v^T \\ 1_v & K + \gamma^{-1}I \end{bmatrix} \begin{bmatrix} b \\ \alpha \end{bmatrix} = \begin{bmatrix} 0 \\ y \end{bmatrix} \quad (23)$$

376 where  $1_v = [1, 1, K, 1]^T$ ,  $\alpha = [\alpha_1, \alpha_2, K, \alpha_n]^T$  and  $y = [y_1, y_2, K, y_m]^T$ .

377 According to the Mercer's condition, the kernel function  $K(x_i, x_j)$ , can be chosen such that

378 
$$K(x_i, x_j) = \phi(x_i)^T \phi(x_j), \quad i, j = 1, 2, \dots, K, n \quad (24)$$

379 This results in the final LSSVM model (Equation (25)) used for estimating the function.

380 
$$f(x) = \sum_{i=1}^n \alpha_i K(x_i, x_j) + b \quad (25)$$

381 where  $\alpha, b$  are solutions to Equation (23).

382 However, it is a widely known fact that the classification accuracy of LSSVM is highly influenced by the  
 383 optimal selection of the kernel function and regularisation parameter. In this paper, the frequently used kernel  
 384 function, the Radial Basis Function (RBF) was selected due to its excellent general performance, wider  
 385 convergence domain, high-resolution power and requires fewer parameters (Keerthi and Lin 2003; Du et al.  
 386 2016; Wang et al. 2018). The RBF kernel function is expressed in Equation (26).

387 
$$RBF = K(x_i, x_j) = \exp\left(-\frac{\|x_i - x_j\|^2}{2\sigma^2}\right) \quad (26)$$

388 For the selection of the optimal bandwidth ( $\sigma$ ) and regularisation ( $\gamma$ ) parameters for an effective  
 389 classification by LSSVM, a hybrid of Coupled Simulated Annealing (CSA) and Nelder-Mead Simplex  
 390 (NMS) optimisation algorithms were adopted to determine the starting points and fine-tune the parameters,  
 391 respectively.

#### 392 4.3.2 Coupled Simulated Annealing (CSA)

393 CSA is an accelerated global optimisation technique characterised by a set of parallel simulated annealing  
 394 processes coupled with their acceptance probability function (Xavier-de-Souza et al. 2009). The introduction  
 395 of a coupling term in CSA allows for the creation of cooperative behaviour through the exchange of  
 396 information which help steer the overall optimisation process toward the global optimum. This minimises the  
 397 sensitivity of the technique to initialisation parameters, thus resulting in a much efficient optimisation.

398 In CSA, the acceptance probability function  $A_\theta(\rho, x_i \rightarrow y_i)$  for every  $x_i \in \Theta$ ,  $y_i \in \Omega$  with coupling term  
 399  $\rho$  is as shown in Equation (27).

400 
$$A_\theta(\rho, x_i \rightarrow y_i) = \frac{\exp\left(\frac{-E(y_i)}{T_k^{ac}}\right)}{\exp\left(\frac{-E(y_i)}{T_k^{uc}}\right) + \rho} \quad (27)$$

401 where  $x_i$  and  $y_i$  are  $i^{th}$  the current state and its corresponding probing state respectively, for  $i = 1, 2, \dots, m$ ,  
 402 with  $m$  being the number of entries in  $\Theta$ . The  $\Theta = \{x_i\}_{i=1}^m$  denotes the set of current states. The coupling  
 403 term  $\rho$ , is a function of the energy of the entries in  $\Theta$  as shown in Equation (28)

404 
$$\rho = \sum_{x \in \{x_1, x_2, \dots, x_m\}} \exp\left(\frac{E(x)}{T_k^{ac}}\right) \quad (28)$$

405 Hence, CSA considers many current states  $x_i = \{x_1, x_2, \dots, x_m\}$  in the set of current states  $\Theta$  and accepts a  
 406 probing state  $y_i = \{y_1, y_2, \dots, y_m\}$  which is not based only on its corresponding  $x_i$  but also on the coupling  
 407 term  $\rho$ . In this paper, CSA is used to determine the starting values of the optimal bandwidth ( $\sigma$ ) and the  
 408 regularisation ( $\gamma$ ) parameters of the LSSVM approach which are then passed on to the NMS technique for  
 409 fine-tuning.

410

### 411 4.3.3 Nelder-Mead Simplex (NMS) Algorithm

412 The NMS algorithm is one of the popular direct search algorithms for optimising multidimensional  
 413 unconstrained problems (Nelder and Mead 1965). Unlike other simplex methods, the NMS algorithm is  
 414 known to be an improvement as it allows the simplex to vary not only in size but as well in shape (Baudin  
 415 2009). The algorithm preserves a simplex (i.e. a geometric figure based on  $n$  parameters defined by  $n+1$   
 416 vertices in  $n+1$  initial experiments) which are approximations of the optimal point. The vertices are sorted  
 417 based on increasing function values from the objective function. The algorithm then tries to replace the worst  
 418 vertex with a new point which is dependent on the worst point and the centre of the best vertices. The  
 419 expansions and contraction operations (varying in size and shape) of the algorithm allows for convergence  
 420 speed which significantly reduces the time complexity.

421 Suppose Equation (29) is an unconstrained optimisation problem

$$422 \quad \min f(x) \quad (29)$$

423 where  $f$  is the objective function with  $x \in \mathbb{R}^n$  and  $n$  as the number of optimisation parameters. The NMS  
 424 algorithm is based on the iterative update of a simplex  $x_i = \{x_1, x_2, \dots, x_{n+1}\}$  which is an  $n \times (n+1)$  matrix  
 425 with each column representing a simplex vertex ( $v_i$ ). The algorithm utilises four major coefficient  
 426 parameters: the reflection ( $\alpha > 0$ ), expansion ( $\beta > 1$ ), contraction ( $0 < \gamma < 1$ ) and shrinkage ( $0 < \sigma < 1$ )  
 427 . The NMS algorithm is presented as follows:

428 **Step 1:** Build  $n+1$  vertices of  $x_i$  such that  $f(x_1) \leq f(x_2) \leq \dots \leq f(x_{n+1})$  .

429 **Step 2:** Use Equation (30) to compute the reflection point  $x_r$

$$430 \quad x_r = \bar{m} + \alpha(\bar{m} - x_{n+1}) \quad (30)$$

431 where  $\bar{m} = \frac{1}{n} \sum_{i=1}^n x_i$  is the centroid of the  $n$  best vertices except  $x_{n+1}$  . If  $f(x_1) \leq f(x_r) < f(x_n)$ , the iteration  
 432 is terminated by accepting  $x_r$  .

433 **Step 3:** If  $f(x_r) < f(x_1)$ , the *expansion* point  $x_e$  is estimated using Equation (31)

$$434 \quad x_e = \bar{m} + \beta(x_r - \bar{m}) \quad (31)$$

435 If  $f(x_e) \leq f(x_r)$ ,  $x_e$  is accepted, else  $x_r$  is accepted while  $x_e$  is discarded and iteration is terminated.

436 **Step 4:** If  $f(x_r) \geq f(x_n)$ , estimate the contraction point between  $\bar{m}$  and the best among  $x_r$  and  $x_{n+1}$

437 i. If  $f(x_r) < f(x_{n+1})$ , an outside contraction point  $x_{cout}$  is estimated using Equation (32)

$$438 \quad x_{cout} = \bar{m} + \gamma(x_r - \bar{m}) \quad (32)$$

439 If  $f(x_{cout}) \leq f(x_r)$ ,  $x_{cout}$  is accepted and iteration is terminated, else skip to Step 5.

440 ii. Elseif  $f(x_r) \geq f(x_{n+1})$ , an inside contraction point  $x_{cin}$  is estimated using Equation (33)

$$441 \quad x_{cin} = \bar{m} + \gamma(x_r - \bar{m}) \quad (33)$$

442 If  $f(x_{cin}) \leq f(x_r)$ ,  $x_{cin}$  is accepted and iteration is terminated, else skip to step 5.

443 **Step 5:**  $f$  is then evaluated at  $n$  points  $v_i = x_1 + \sigma(x_i - x_1)$ , for every  $i = 2, K, n+1$ . For the next iteration,  
444 the vertices  $v_i$  are assigned to  $x_i$ .

445 The standard values for the four major coefficient parameters:  $x_r = 1$ ,  $x_e = 2$ ,  $x_r = \frac{1}{2}$  and  $\sigma = \frac{1}{2}$ .

446 The optimal bandwidth ( $\sigma$ ) and regularisation ( $\gamma$ ) parameters proposed and refined by the combination of  
447 CSA and NMS algorithms are then passed on to LSSVM to facilitate the classification.

#### 448 **4.4 Classification performance evaluation**

449 From the statistical viewpoint, deducing a comprehensive evaluation of multiclass classification models based  
450 on a single performance index is not easy and enough. For these reasons, eight evaluation metrics namely  
451 accuracy, error rate, precision, recall (sensitivity), specificity, F score, Mathews correlation coefficient and  
452 geometric mean were used in this study for the purpose of reliability and also to overcome the above  
453 drawback.

##### 454 **4.4.1 Accuracy**

455 Accuracy is one of the most widely used evaluation metrics for assessing the performance of classification  
456 algorithms (Paul and Maji 2010; Qasem and Nour 2015; Alsalem et al. 2018). Classification accuracy is  
457 expressed in Equation (34) as

$$458 \text{Accuracy} = \frac{TP + TN}{TP + FP + TN + FN} \quad (34)$$

459 where  $TP$  is the number of correct classification counts when there is a fault condition,  $TN$  is the number  
460 of correct classification counts when there is no fault condition,  $FP$  is the number of misclassification counts  
461 when there is a fault condition and  $FN$  is the number of misclassification counts when there is no fault  
462 condition for a specific classification model.

##### 463 **4.4.2 Error rate**

464 This metric is one of the main indicators for evaluating classification performance by measuring the errors  
465 (misclassifications) incurred by a classifier (Chiang and Ho 2008; De Paz et al. 2013; Mohapatra and  
466 Chakravarty 2015; Alsalem et al. 2018). The error rate is expressed as shown in Equation (35).

$$467 \text{Error Rate} = \frac{FP + FN}{TP + FP + TN + FN} \quad (35)$$

##### 468 **4.4.3 Precision**

469 The precision of a classifier measures the exactness of classification after prediction (Agaian et al. 2014;  
470 Mohapatra and Chakravarty 2015; Alsalem et al. 2018). The evaluation metric is expressed as a ratio of true  
471 positives ( $TP$ ) to the sum of true positives ( $TP$ ) and false positives ( $FP$ ) as shown in Equation (36).

$$472 \text{Precision} = \frac{TP}{TP + FP} \quad (36)$$

##### 473 **4.4.4 Recall (Sensitivity)**

474 Recall, also known as sensitivity, is a measure of a classifier's capacity to determine positive instances. It  
475 measures the fraction of positive instances that are correctly classified (Agaian et al. 2014; Tai et al. 2011;  
476 Alsalem et al. 2018) and is expressed as a ratio of true positives ( $TP$ ) to the sum of true positives ( $TP$ ) and  
477 false negatives ( $FN$ ) as shown in Equation (37).

$$478 \text{Recall / Sensitivity} = \frac{TP}{TP + FN} \quad (37)$$

#### 479 4.4.5 Specificity

480 Specificity measures the fraction of negative instances that are correctly classified (Agaian et al. 2014; Laosai  
481 and Chamnongthai 2014). That is, the metric denotes the test's ability to identify negative result as expressed  
482 in Equation (38).

$$483 \text{Specificity} = \frac{TN}{TN + FP} \quad (38)$$

#### 484 4.4.6 F score

485 The F Score describes the overall performance of a classification model as the harmonic mean of precision  
486 and recall (Agaian et al. 2014; Mohapatra and Chakravarty 2015; Alsalem et al. 2018). The metric ranges  
487 from zero to one, with high values indicating high classification performance and vice versa. F Score is given  
488 in Equation (39).

$$489 \text{FScore} = \frac{2(\text{Precision} * \text{Recall})}{\text{Precision} + \text{Recall}} \quad (39)$$

#### 490 4.4.7 Matthews Correlation Coefficient (MCC)

491 MCC (Equation (40)) measures the relationship between the observed and the predicted classification and is  
492 generally regarded as a balanced metric for evaluating the performance of classifiers even with varying class  
493 sizes (Boughorbel et al. 2017; Chicco 2017). MCC, as compared to other classification evaluation metrics is  
494 known to be more informative as it considers the balance ratios of the four confusion matrix categories. An  
495 MCC coefficient ranges from -1 to +1, with +1 suggesting a perfect classification while -1 implies a total  
496 misclassification.

$$497 \text{MCC} = \frac{(TP * TN) - (FP * FN)}{\sqrt{(TP + FP)(TP + FN)(TN + FP)(TN + FN)}} \quad (40)$$

#### 498 4.4.8 Geometric Mean (GM)

499 GM (Equation (41)) is an aggregate of both sensitivity and specificity evaluation metrics. The metric seeks  
500 to maximise the rate of true positives and negatives instances while maintaining a balance between both  
501 rates (Hossin and Sulaiman 2015; Kuncheva et al. 2018). Thus, making the metric suitable for imbalanced  
502 datasets.

$$503 \text{GM} = \sqrt{\frac{TP}{TP + FN} * \frac{TN}{TN + FP}} \quad (41)$$

## 504 5 Results and discussion

### 505 5.1 Data pre-processing

#### 506 5.1.1 Denoising

507 The hydraulic system dataset was first subjected to the modified ICEEMDAN technique (integrated with the  
508 stringent threshold (Equation (8)) as a criterion for discriminating between relevant and spurious IMFs) as  
509 discussed in Section 4.1.2. The modification was automated such that, the denoising (decomposition into  
510 IMFs with ICEEMDAN and reconstruction with Equation (8)) was repeated for all the sensors considered in  
511 this study as manual involvement was highly impractical. The modified ICEEMDAN technique successfully  
512 eliminated most redundancies masked as noise in the sensor data.

#### 513 5.1.2 Feature extraction and selection

514 Here, two different data scenarios were considered when applying the PCA. First, the PCA was applied to  
515 the resulting pool of 1806 features which have been denoised using the ICEEMDAN technique. Secondly,  
516 the PCA was applied directly to the original extracted 1806 features without denoising. The motive is to  
517 ascertain the extent to which the denoised data could improve the classifiers prediction capability. Fig. 4(a)  
518 shows the scree plot of the eigenvalues and the proportion of variance explained regarding the undenoised

519 1806 possible components while Fig. 4(b) shows the PCA results for the denoised 1806 features. Using the  
520 Kaiser's criterion for retaining PCs with eigenvalues greater than 1.0, 161 PCs were retained for the  
521 undenoised data representing 91.62% of the variance in the 1806 features. With regards to the denoised data  
522 using the ICEEMDAN, the number of selected PCs was substantially reduced by half (82) when compared  
523 to the undenoised data, representing 96.04% of the variance in the 1806 features as shown in Table 3. The  
524 results from both approaches (with and without the use of ICEEMDAN) clearly indicate the relevance of the  
525 ICEEMDAN technique in removing substantial levels of noise in the original hydraulic sensor data before  
526 feature extraction and selection. Thus, ensuring the extraction of relevant features that contains the most  
527 characteristic fault information projected onto a minimal number of uncorrelated PCs while maintaining a  
528 high proportion of variance (96.04%) during the dimensionality reduction phase.

## 529 **5.2 Multiclass classification**

530 Multiclass classification refers to classifying input features to one of a predefined set based on an optimal  
531 subset of features selected during the feature selection stage. In this study, the multiclass classification model  
532 result of the optimised LSSVM was compared with three benchmark machine learning techniques that have  
533 been used extensively in literature and have all demonstrated promising multiclass classification capabilities.  
534 The methods include Linear Discriminant Analysis (LDA), Support Vector Machine (SVM) and Artificial  
535 Neural Network (ANN), specifically, the Generalised Regression Neural Network (GRNN). If the  
536 performance of the tested classification model is deemed satisfactory, the classification model can be used to  
537 classify the unknown future health status of the hydraulic component. Fig. 5 shows the illustration of the  
538 procedure used in building the multiclass classification models. The classification experiment was simulated  
539 on MATLAB (2018a version) using an ASUS computer with a 2.3 GHz processor computer with 4 GB  
540 memory.

541 In order to ascertain the reliability of the multiclass classification models, the selected features from PCA are  
542 randomly partitioned into two sets; 70% (training set) to be used in training the multiclass classification  
543 models and the 30% (testing set) is used to validate the optimum trained models. However, the random nature  
544 of the hybrid CSA-NMS optimisation algorithms in providing the optimal bandwidth and the regularisation  
545 parameters of the LSSVM will yield slightly different output after each run. As a result, the LSSVM is  
546 implemented using the one-vs-one with RBF kernel, and is trained 10 times based on randomly partitioned  
547 data into training and test sets. The final classification output is presented as an average, standard deviation  
548 (STD), best and worst of all the outputs from the 10 runs as shown in Table 4. Notably, the proposed hybrid  
549 technique achieved average test classification accuracies greater than 99.40% for all four monitored conditions.  
550 Also found in Table 4 is the training accuracy, its deviation (10-fold cross-validation) and CPU time regarding  
551 the training of LSSVM optimised by CSA-NMS for the four hydraulic components.

### 552 **5.2.1 Classification rate based on optimised LSSVM compared to other investigated classifiers**

553 Table 5 shows the average multiclass classification test results for hydraulic accumulator condition based on  
554 pre-processed ICEEMDAN-PCA and PCA input features for the optimised LSSVM, LDA, SVM and ANN.  
555 Although all the classifiers showed satisfactory test performance, the proposed ICEEMDAN-PCA-LSSVM  
556 outperformed all the other methods. This is evident from the various evaluation metrics employed (Table 5).  
557 The performance (99.44%) by the proposed technique in classifying the accumulator condition is remarkably  
558 significant when compared to the results reported in prior work after classification based LDA (54.0%), ANN  
559 (50.4%), SVM-linear (51.6%) and SVM-RBF (65.7%) (Helwig et al. 2015a). Also, another prior work  
560 conducted by Chawathe (2019) reported similar classification results ranging from >35% to <100% based on  
561 seven different classifiers/ensemble. In prior works, the classification of accumulator condition is reported as  
562 the most difficult among the four monitored components (Helwig et al. 2015a; Chawathe 2019). Hence, the  
563 proposed hybrid model of ICEEMDAN-PCA-LSSVM demonstrates superiority of producing a more accurate  
564 classification of the hydraulic accumulator condition.

565 Also seen in Table 5 is a comparative analysis of the proposed ICEEMDAN-PCA-LSSVM with its variant,  
566 undenoised PCA-LSSVM. The comparative analysis is performed to assess the contribution of the  
567 ICEEMDAN to the proposed hybrid technique. As seen, the proposed ICEEMDAN-PCA-LSSVM model  
568 accurately classified 99.44% of the test instances with an error of 0.56% as compared to the 94.09% accuracy  
569 with 5.91% misclassification rate (error) in the case of not using ICEEMDAN to pre-process the data (i.e.

570 PCA-LSSVM). This suggests that pre-processing (denoising) the original signals with ICEEMDAN  
571 improved the proposed hybrid technique by 5.35%. In terms of precision, the proposed ICEEMDAN-PCA-  
572 LSSVM was capable of classifying 99.56% of the positive instances correctly out of the total test instances  
573 while the PCA-LSSVM technique could only classify 93.03% of positive instances. Also, the highest  
574 sensitivity and specificity values of 0.9941 and 0.9980 imply the proposed models' (ICEEMDAN-PCA-  
575 LSSVM) ability to determine 99.41% of all positive instances and 99.80% of all negative instances,  
576 respectively. The sensitivity and specificity values of the PCA-LSSVM technique, on the other hand, could  
577 classify only 93.33% and 98.10% of positive and negative instances respectively. This suggests that the  
578 proposed ICEEMDAN-PCA-LSSVM model has high potency for differentiating positive instances from  
579 negative instances. Furthermore, the ICEEMDAN-PCA-LSSVM model demonstrated the highest f-score of  
580 0.9948 as compared to the 0.9317 of the PCA-LSSVM technique regarding overall performance of  
581 classification. A correlation coefficient of 0.9929 and 0.9126 for ICEEMDAN-PCA-LSSVM and PCA-  
582 PSSVM implies a positive relationship between the classified and the observed test instances for both  
583 techniques. However, it was stronger for the proposed ICEEMDAN-PCA-LSSVM model. All these  
584 evaluation metrics along with a high geometric mean value of 0.9960 collectively suggest nearly perfect  
585 classification results for accumulator condition is achieved using the proposed hybrid model of ICEEMDAN-  
586 PCA-LSSVM.

587 In the case of the cooler condition, similar average multiclass classification test results as in the accumulator  
588 condition were obtained (Table 6). However, the classification results obtained by the proposed ICEEMDAN-  
589 PCA-LSSVM, ICEEMDAN-PCA-ANN and PCA-LSSVM models were quite similar. That is, these models  
590 achieved the same highest level of accuracy (99.83%) with a corresponding lowest misclassification rate  
591 (error) of 0.17%. Similar results were obtained for the remaining evaluation metrics considered. The  
592 interpretation here is that the proposed ICEEMDAN-PCA-LSSVM model can adequately be used in  
593 classifying cooler conditions.

594 Table 7 shows the average multiclass classification test results for internal pump leakage condition. As  
595 observed in Table 7, the ICEEMDAN based classification with LSSVM and SVM models showed better  
596 accuracy and generalisability. This is evident from the perfect test classification results (100%) obtained by  
597 both the proposed hybrid model (ICEEMDAN-PCA-LSSVM) and the ICEEMDAN-PCA-SVM model.  
598 These 100% test classification results obtained by the proposed technique is seen to be a significant  
599 improvement to prior works of classification based LDA (73.6%), ANN (80.0%), SVM-linear (72.4%) and  
600 SVM-RBF (64.2%) (Helwig et al. 2015a). Also, similar classification results ranging from >55% to <100%  
601 based on seven different classifiers/ensemble was obtained by Chawathe (2019). Deductions from prior works  
602 indicate the classification of the pump condition to be the next most difficult after the accumulator condition  
603 (Helwig et al. 2015a; Chawathe 2019). This suggests that the proposed hybrid model of ICEEMDAN-PCA-  
604 LSSVM and ICEEMDAN-PCA-SVM are optimal for the accurate classification of internal pump leakage  
605 condition.

606 With regards to the average multiclass classification of the valve conditions (Table 8), the proposed  
607 ICEEMDAN-PCA-LSSVM model showed better classification results than the alternative models. This is  
608 manifested in the 99.84% accuracy with a 0.16% misclassification (error) rate obtained. The same trend of  
609 results was noticed for the remaining evaluation metrics considered (Table 8). Here, the proposed  
610 ICEEMDAN-PCA-LSSVM model is considered to be suitable in classifying the valve condition of the  
611 hydraulic system.

612 The overall analyses of all the multiclass classification results of the various fault conditions (accumulator,  
613 cooler, pump leakage and valve) have shown the superiority of the ICEEMDAN-PCA-LSSVM proposed.  
614 This is because the ICEEMDAN-PCA-LSSVM is able to classify all the fault conditions better than the other  
615 methods. Hence, the method possesses the added advantage of being versatile in multiclass classification  
616 tasks as observed in this study for the various monitored conditions. Methods such as ICEEMDAN-PCA-  
617 ANN and PCA-LSSVM which achieved relatively similar classification results could only do so in the case  
618 of cooler conditions (Table 6) while ICEEMDAN-PCA-SVM only classified the internal pump leakage  
619 correctly (see Table 7). These suggest that the proposed ICEEMDAN-PCA-LSSVM model is highly potent  
620 in classifying a wide range of monitored conditions irrespective of the dynamic operational condition of the

621 machine component. This will aid machine operators to spot significant changes in machine components  
622 which is an indication of fault development. Thus, increasing the availability and reliability of machines, as  
623 well as reducing maintenance-related cost by presenting operators with an accurate and informed decision as  
624 to when to schedule maintenance.

625 Furthermore, this study has practically demonstrated the relevance of denoising the original signals by the  
626 ICEEMDAN technique to enhance the overall classification results. This is evident in the results presented  
627 in Tables 5 - 8 where two scenarios of denoising the originally recorded data using ICEEMDAN and using  
628 the originally recorded data without denoising in the modelling process. The strength of the proposed  
629 modelling approach (ICEEMDAN-PCA-LSSVM) can additionally be viewed from Figs. 6 and 7. Here, only  
630 the PCA-LSSVM was chosen to be compared with the proposed ICEEMDAN-PCA-LSSVM model because  
631 it was the best of the models based on undenoised features. Considering the relevance of denoising the signals  
632 with ICEEMDAN hybridised with PCA and LSSVM for improving the classification of diverse monitored  
633 conditions, it may be limited when experimented on signals with mutations and similar dominant frequencies.

## 634 **6 Conclusions**

635 In this study, a hybrid approach based on the ICEEMDAN, PCA and LSSVM optimised by CSA-NMS for  
636 multiclass fault classification has been developed and evaluated. In ascertaining the superiority of the  
637 proposed hybrid approach (ICEEMDAN-PCA-LSSVM), a comparative analysis with three well-established  
638 benchmark classifiers (i.e. LDA, SVM and ANN) was carried out using benchmark data obtained from multi-  
639 sensors of a hydraulic test rig. From the analysis of the results, it was found that the proposed hybrid  
640 ICEEMDAN-PCA-LSSVM model was versatile and had the best results across all the performance indicators  
641 leading to better diagnostic of various fault conditions. The proposed hybrid approach also had the tendency  
642 of reducing the redundancies and the dimension of features thereby allowing for the efficient consideration  
643 of relevant features for the enhancement of classification accuracy and convergence speed. Hence, the  
644 proposed hybrid technique possesses the added advantage of being versatile in classifying various monitored  
645 conditions. The compared classifiers achieved relatively similar classification performance; however, they  
646 could only do so in the case of the cooler and the internal pump leakage. These suggest that the proposed  
647 hybrid is highly potent in classifying a wide range of monitored conditions irrespective of the dynamic  
648 operational conditions. Although the proposed hybrid technique generally improves the classification of  
649 diverse monitored conditions, it may be limited when experimented on signals with mutations and similar  
650 dominant frequencies. Also, the feature extraction technique as well as those utilised in prior research works  
651 may be constrained when dealing with extremely larger datasets due to the level of manual involvement by  
652 the user. Hence, future works should explore the following: the usage of filters capable of addressing signals  
653 with mutation and similar dominant frequencies, deep learning approaches to feature extraction. This will  
654 ultimately improve the optimality of the pre-processed signals for various fault classification tasks in the field  
655 of predictive maintenance.

656 **Conflict of Interest:** The authors declare that they have no conflict of interest.

## 657 **References**

- 658 Agaian S, Madhukar M, Chronopoulos AT (2014) Automated screening system for acute myelogenous  
659 leukemia detection in blood microscopic images. *IEEE Systems journal* 8:995–1004
- 660 Alsalem MA, Zaidan AA, Zaidan BB, et al (2018) Systematic review of an automated multiclass detection  
661 and classification system for acute Leukaemia in terms of evaluation and benchmarking, open  
662 challenges, issues and methodological aspects. *Journal of medical systems* 42:204
- 663 Ayenu-Prah A, Attoh-Okine N (2010) A criterion for selecting relevant intrinsic mode functions in empirical  
664 mode decomposition. *Advances in Adaptive Data Analysis* 2:1–24
- 665 Bach F (2017) Breaking the curse of dimensionality with convex neural networks. *Journal of Machine*  
666 *Learning Research* 18:1–53
- 667 Barschdorff D, Femmer U (1995) Signal processing and pattern recognition methods for biomedical sound  
668 analysis. In: *2nd International Symposium Acoustical and Vibratory Surveillance Methods and*  
669 *Diagnostic Techniques*. p 279

- 670 Baudin M (2009) Nelder mead user's manual. Digiteo
- 671 Boughorbel S, Jarray F, El-Anbari M (2017) Optimal classifier for imbalanced data using Matthews  
672 Correlation Coefficient metric. *PloS one* 12:e0177678
- 673 Casoli P, Pastori M, Scolari F, Rundo M (2019) A vibration signal-based method for fault identification and  
674 classification in hydraulic axial piston pumps. *Energies* 12:953
- 675 Chakraborty T (2017) EC3: Combining Clustering and Classification for Ensemble Learning. In: 2017 IEEE  
676 International Conference on Data Mining (ICDM). pp 781–786
- 677 Chawathe SS (2019) Condition monitoring of hydraulic systems by classifying sensor data streams. In: 2019  
678 IEEE 9th Annual Computing and Communication Workshop and Conference (CCWC). IEEE, pp  
679 0898–0904
- 680 Cheng Y, Wang Z, Chen B, et al (2019) An improved complementary ensemble empirical mode  
681 decomposition with adaptive noise and its application to rolling element bearing fault diagnosis. *ISA*  
682 *transactions*
- 683 Chiang J-H, Ho S-H (2008) A combination of rough-based feature selection and RBF neural network for  
684 classification using gene expression data. *IEEE transactions on nanobioscience* 7:91–99
- 685 Chicco D (2017) Ten quick tips for machine learning in computational biology. *BioData mining* 10:35
- 686 Cho M-Y, Hoang TT (2017) Feature selection and parameters optimization of svm using particle swarm  
687 optimization for fault classification in power distribution systems. *Computational intelligence and*  
688 *neuroscience* 2017:
- 689 Cho S, May G, Tourkogiorgis I, et al (2018) A Hybrid Machine Learning Approach for Predictive  
690 Maintenance in Smart Factories of the Future. In: *IFIP International Conference on Advances in*  
691 *Production Management Systems*. Springer, pp 311–317
- 692 Çınar ZM, Abdussalam Nuhu A, Zeeshan Q, et al (2020a) Machine learning in predictive maintenance  
693 towards sustainable smart manufacturing in industry 4.0. *Sustainability* 12:8211
- 694 Çınar ZM, Abdussalam Nuhu A, Zeeshan Q, et al (2020b) Machine Learning in Predictive Maintenance  
695 towards Sustainable Smart Manufacturing in Industry 4.0. *Sustainability* 12:8211.  
696 <https://doi.org/10.3390/su12198211>
- 697 Cohen L (1989) Time-frequency distributions-a review. *Proceedings of the IEEE* 77:941–981
- 698 Colominas MA, Schlotthauer G, Torres ME (2014) Improved complete ensemble EMD: A suitable tool for  
699 biomedical signal processing. *Biomedical Signal Processing and Control* 14:19–29
- 700 Daubechies I (1989) Orthonormal bases of wavelets with finite support—connection with discrete filters. In:  
701 *Wavelets*. Springer, pp 38–66
- 702 De Paz JF, Bajo J, López VF, Corchado JM (2013) Biomedic Organizations: An intelligent dynamic  
703 architecture for KDD. *Information Sciences* 224:49–61
- 704 Di Z, Kang Q, Peng D, Zhou M (2019) Density Peak-based Pre-clustering Support Vector Machine for Multi-  
705 class Imbalanced Classification. In: 2019 IEEE International Conference on Systems, Man and  
706 Cybernetics (SMC). pp 27–32
- 707 Dorigo M, Birattari M, Stutzle T (2006) Ant colony optimization. *IEEE Computational Intelligence Magazine*  
708 1:28–39. <https://doi.org/10.1109/MCI.2006.329691>
- 709 Du D, Jia X, Hao C (2016) A New Least Squares Support Vector Machines Ensemble Model for Aero Engine  
710 Performance Parameter Chaotic Prediction. *Mathematical Problems in Engineering* 2016:
- 711 Egusquiza M, Egusquiza E, Valero C, et al (2018) Advanced condition monitoring of Pelton turbines.  
712 *Measurement* 119:46–55
- 713 Galli AW, Heydt GT, Ribeiro PF (1996) Exploring the power of wavelet analysis. *IEEE Computer*  
714 *Applications in Power* 9:37–41
- 715 Gomes JP, Rodrigues LR, Leao BP, et al (2016) Using degradation messages to predict hydraulic system  
716 failures in a commercial aircraft. *IEEE Transactions on Automation Science and Engineering*  
717 15:214–224

- 718 Haddar M (2018) L-Kurtosis and Improved Complete Ensemble EMD in Early Fault Detection Under  
719 Variable Load and Speed. In: *Advances in Acoustics and Vibration II: Proceedings of the Second*  
720 *International Conference on Acoustics and Vibration (ICAV2018)*, March 19-21, 2018, Hammamet,  
721 Tunisia. Springer, p 3
- 722 Hao W, Dong Y, Cai Y (2020) Design of Safety Monitoring System for Stage Machinery System. In: 2020  
723 IEEE International Conference on Artificial Intelligence and Computer Applications (ICAICA). pp  
724 320–324
- 725 Har-Peled S, Indyk P, Motwani R (2012) Approximate nearest neighbor: Towards removing the curse of  
726 dimensionality. *Theory of computing* 8:321–350
- 727 Hathaway BJ, Garde K, Mantell SC, Davidson JH (2018) Design and characterization of an additive  
728 manufactured hydraulic oil cooler. *International Journal of Heat and Mass Transfer* 117:188–200
- 729 Helwig N, Pignanelli E, Schütze A (2015a) Condition monitoring of a complex hydraulic system using  
730 multivariate statistics. In: *Instrumentation and Measurement Technology Conference (I2MTC),*  
731 2015 IEEE International. IEEE, pp 210–215
- 732 Helwig N, Pignanelli E, Schütze A (2015b) Detecting and Compensating Sensor Faults in a Hydraulic  
733 Condition Monitoring System. In: *In proceeding Sensor. SENSOR*, pp 641–646
- 734 Herrmann FJ, Friedlander MP, Yilmaz O (2012) Fighting the curse of dimensionality: Compressive sensing  
735 in exploration seismology. *IEEE Signal Process Mag* 29:88–100
- 736 Hlawatsch F, Boudreaux-Bartels GF (1992) Linear and quadratic time-frequency signal representations. *IEEE*  
737 *signal processing magazine* 9:21–67
- 738 Hossin M, Sulaiman MN (2015) A review on evaluation metrics for data classification evaluations.  
739 *International Journal of Data Mining & Knowledge Management Process* 5:1
- 740 Houle ME, Kriegel H-P, Kröger P, et al (2010) Can shared-neighbor distances defeat the curse of  
741 dimensionality? In: *International Conference on Scientific and Statistical Database Management.*  
742 Springer, pp 482–500
- 743 Huang NE, Shen Z, Long SR, et al (1998) The empirical mode decomposition and the Hilbert spectrum for  
744 nonlinear and non-stationary time series analysis. *Proceedings of the Royal Society of London Series*  
745 *A: Mathematical, Physical and Engineering Sciences* 454:903–995
- 746 Ilonen J, Kamarainen J-K, Lampinen J (2003) Differential Evolution Training Algorithm for Feed-Forward  
747 Neural Networks. *Neural Processing Letters* 17:93–105. <https://doi.org/10.1023/A:1022995128597>
- 748 Javed K (2014) A robust & reliable Data-driven prognostics approach based on extreme learning machine  
749 and fuzzy clustering. PhD Thesis
- 750 Karaboga D, Gorkemli B, Ozturk C, Karaboga N (2014) A comprehensive survey: artificial bee colony (ABC)  
751 algorithm and applications. *Artif Intell Rev* 42:21–57. <https://doi.org/10.1007/s10462-012-9328-0>
- 752 Karanović V, Jocanović M, Baloš S, et al (2019) Impact of contaminated fluid on the working performances  
753 of hydraulic directional control valves. *Journal of Mechanical Engineering*
- 754 Kaur H, Kaur M (2020) Fault Classification in a Transmission Line Using Levenberg–Marquardt Algorithm  
755 Based Artificial Neural Network. In: *Data Communication and Networks*. Springer, pp 119–135
- 756 Keerthi SS, Lin C-J (2003) Asymptotic behaviors of support vector machines with Gaussian kernel. *Neural*  
757 *computation* 15:1667–1689
- 758 Kennedy J, Eberhart R (1995) Particle swarm optimization. In: *Proceedings of ICNN'95 - International*  
759 *Conference on Neural Networks*. pp 1942–1948 vol.4
- 760 Keogh E, Mueen A (2011) Curse of dimensionality. In: *Encyclopedia of machine learning*. Springer, pp 257–  
761 258
- 762 König C, Helmi AM (2020) Sensitivity Analysis of Sensors in a Hydraulic Condition Monitoring System  
763 Using CNN Models. *Sensors* 20:3307. <https://doi.org/10.3390/s20113307>
- 764 Kuncheva LI, Arnaiz-González Á, Díez-Pastor J-F, Gunn IAD (2018) Instance Selection Improves Geometric  
765 Mean Accuracy: A Study on Imbalanced Data Classification. arXiv:180407155 [cs, stat]

- 766 Laosai J, Chamnongthai K (2014) Acute leukemia classification by using SVM and K-Means clustering. 2014  
767 International Electrical Engineering Congress (iEECON) 1–4.  
768 <https://doi.org/10.1109/ieecon.2014.6925840>
- 769 Lei Y, Jiang W, Jiang A, et al (2019) Fault diagnosis method for hydraulic directional valves integrating PCA  
770 and XGBoost. *Processes* 7:589
- 771 Leon-Quiroga J, Newell B, Krishnamurthy M, et al (2020) Energy Efficiency Comparison of Hydraulic  
772 Accumulators and Ultracapacitors. *Energies* 13:1632
- 773 Mahgoun H, Chaari F, Felkaoui A, Haddar M (2018) L-Kurtosis and Improved Complete Ensemble EMD in  
774 Early Fault Detection Under Variable Load and Speed. In: *International Conference on Acoustics  
775 and Vibration*. Springer, pp 3–15
- 776 Marwala T (2012) *Condition monitoring using computational intelligence methods: applications in  
777 mechanical and electrical systems*. Springer Science & Business Media
- 778 Mohapatra P, Chakravarty S (2015) Modified PSO based feature selection for Microarray data classification.  
779 In: *2015 IEEE Power, Communication and Information Technology Conference (PCITC)*. IEEE, pp  
780 703–709
- 781 Mosavi A, Edalatifar M (2018) A Hybrid Neuro-Fuzzy Algorithm for Prediction of Reference  
782 Evapotranspiration. In: *International Conference on Global Research and Education*. Springer, pp  
783 235–243
- 784 Nelder JA, Mead R (1965) A simplex method for function minimization. *The computer journal* 7:308–313
- 785 Newland DE (2005) *An Introduction to Random Vibrations, Spectral & Wavelet Analysis: Third Edition,  
786 Third edition*. Dover Publications, Mineola, N.Y
- 787 Niu G, Shang F, Krishnamurthy M, Garcia JM (2016) Evaluation and selection of accumulator size in electric-  
788 hydraulic hybrid (EH2) powertrain. In: *2016 IEEE Transportation Electrification Conference and  
789 Expo (ITEC)*. IEEE, pp 1–6
- 790 Paul S, Maji P (2010) Rough set based gene selection algorithm for microarray sample classification. In: *2010  
791 International Conference on Methods and Models in Computer Science (ICM2CS-2010)*. IEEE, pp  
792 7–13
- 793 Peppin RJ (1994) *An Introduction to Random Vibrations, Spectral and Wavelet Analysis*. Hindawi
- 794 Pfeffer A, Glück T, Kemmetmüller W, Kugi A (2016) Mathematical modelling of a hydraulic accumulator  
795 for hydraulic hybrid drives. *Mathematical and Computer Modelling of Dynamical Systems* 22:397–  
796 411
- 797 Pugin KG (2020) Improving the reliability of hydraulic systems of technological machines. *IOP Conf Ser:  
798 Mater Sci Eng* 971:052042. <https://doi.org/10.1088/1757-899X/971/5/052042>
- 799 Qasem M, Nour M (2015) Improving Accuracy for Classifying Selected Medical Datasets with Weighted  
800 Nearest Neighbors and Fuzzy Nearest Neighbors Algorithms. In: *2015 International Conference on  
801 Cloud Computing (ICCC)*. IEEE, pp 1–9
- 802 Quatrini E, Costantino F, Pocci C, Tronci M (2020) Predictive model for the degradation state of a hydraulic  
803 system with dimensionality reduction. *Procedia Manufacturing* 42:516–523
- 804 Randall RB, Antoni J (2011) Rolling element bearing diagnostics—A tutorial. *Mechanical systems and signal  
805 processing* 25:485–520
- 806 Raptodimos Y, Lazakis I (2018) Using artificial neural network-self-organising map for data clustering of  
807 marine engine condition monitoring applications. *Ships and Offshore Structures* 13:649–656
- 808 Rashedi E, Nezamabadi-Pour H, Saryazdi S (2009) GSA: a gravitational search algorithm. *Information  
809 sciences* 179:2232–2248
- 810 Sarkar C (2015) *Improving Predictive Modeling in High Dimensional, Heterogeneous and Sparse Health  
811 Care Data*
- 812 Schneider T, Helwig N, Schütze A (2018) Automatic feature extraction and selection for condition monitoring  
813 and related datasets. In: *2018 IEEE International Instrumentation and Measurement Technology  
814 Conference (I2MTC)*. IEEE, pp 1–6

815 Schneider T, Helwig N, Schütze A (2017) Automatic feature extraction and selection for classification of  
816 cyclical time series data. *tm-Technisches Messen* 84:198–206

817 Sheng C, Li Z, Qin L, et al (2011) Recent progress on mechanical condition monitoring and fault diagnosis.  
818 *Procedia Engineering*, 15, 142-146. 15:142–146

819 Suykens JA, Vandewalle J (1999) Least squares support vector machine classifiers. *Neural processing letters*  
820 9:293–300

821 Suykens JAK, Gestel TV, De Brabanter J, et al (2002) Least squares support vector machines. *World*  
822 *Scientific*

823 Tai W-L, Hu R-M, Hsiao HC, et al (2011) Blood cell image classification based on hierarchical SVM. In:  
824 2011 IEEE International Symposium on Multimedia. IEEE, pp 129–136

825 Torres ME, Colominas MA, Schlotthauer G, Flandrin P (2011) A complete ensemble empirical mode  
826 decomposition with adaptive noise. In: 2011 IEEE international conference on acoustics, speech and  
827 signal processing (ICASSP). IEEE, pp 4144–4147

828 Vianna WOL, de Souza Ribeiro LG, Yoneyama T (2015) Electro hydraulic servovalve health monitoring  
829 using fading extended Kalman filter. In: 2015 IEEE Conference on Prognostics and Health  
830 Management (PHM). IEEE, pp 1–6

831 Wang K, Wen X, Hou D, et al (2018) Application of Least-Squares Support Vector Machines for Quantitative  
832 Evaluation of Known Contaminant in Water Distribution System Using Online Water Quality  
833 Parameters. *Sensors* 18:938

834 Wang L (2017) Heterogeneous Data and Big Data Analytics. *Automatic Control and Information Sciences*  
835 3:8–15. <https://doi.org/10.12691/acis-3-1-3>

836 Wang X, Lin S, Wang S (2016) Remaining useful life prediction model based on contaminant sensitivity for  
837 aviation hydraulic piston pump. In: 2016 IEEE International Conference on Aircraft Utility Systems  
838 (AUS). IEEE, pp 266–272

839 Wen X (2011) A hybrid intelligent technique for induction motor condition monitoring. PhD Thesis,  
840 University of Portsmouth

841 Whitley D (1994) A genetic algorithm tutorial. *Stat Comput* 4:65–85. <https://doi.org/10.1007/BF00175354>

842 Wigner EP (1932) On the quantum correction for thermodynamic equilibrium. In: Part I: Physical Chemistry.  
843 Part II: Solid State Physics. Springer, pp 110–120

844 Wu Z, Huang NE (2009) Ensemble empirical mode decomposition: a noise-assisted data analysis method.  
845 *Advances in adaptive data analysis* 1:1–41

846 Xavier-de-Souza S, Suykens JA, Vandewalle J, Bollé D (2009) Coupled simulated annealing. *IEEE*  
847 *Transactions on Systems, Man, and Cybernetics, Part B (Cybernetics)* 40:320–335

848 Xu G, Ma C, Gao Z, et al (2017a) Modeling and simulation of aero-hydraulic pump wear failure. In: 2017  
849 Prognostics and System Health Management Conference (PHM-Harbin). IEEE, pp 1–7

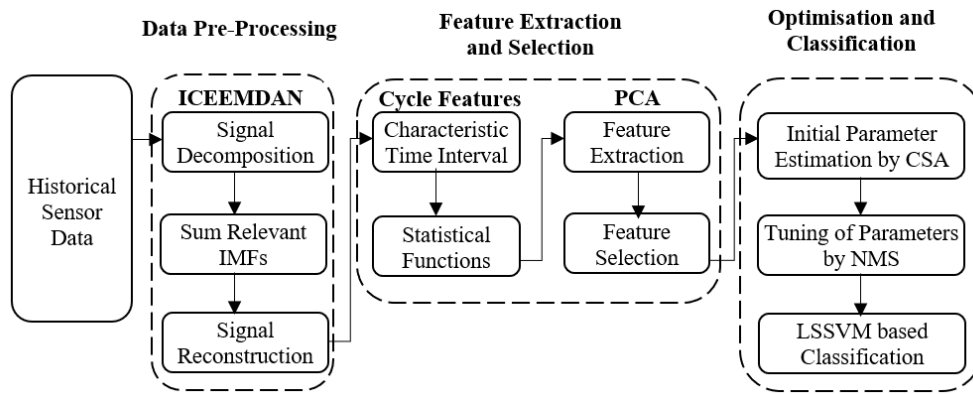
850 Xu G, Ma C, Gao Z, et al (2017b) Modeling and simulation of aero-hydraulic pump wear failure. In: 2017  
851 Prognostics and System Health Management Conference (PHM-Harbin). IEEE, pp 1–7

852 Zhang J, Guo Y, Shen Y, et al (2018) Improved CEEMDAN–wavelet transform de-noising method and its  
853 application in well logging noise reduction. *Journal of Geophysics and Engineering* 15:775–787

854 Zhang X-Y, Yang P, Zhang Y-M, et al (2014) Combination of classification and clustering results with label  
855 propagation. *IEEE Signal Processing Letters* 21:610–614

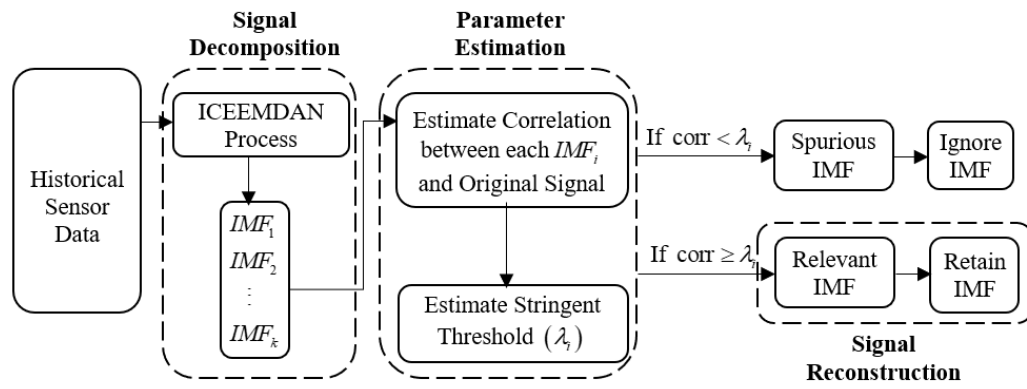
856 Zhang Y, Randall RB (2009) Rolling element bearing fault diagnosis based on the combination of genetic  
857 algorithms and fast kurtogram. *Mechanical Systems and Signal Processing* 23:1509–1517

858



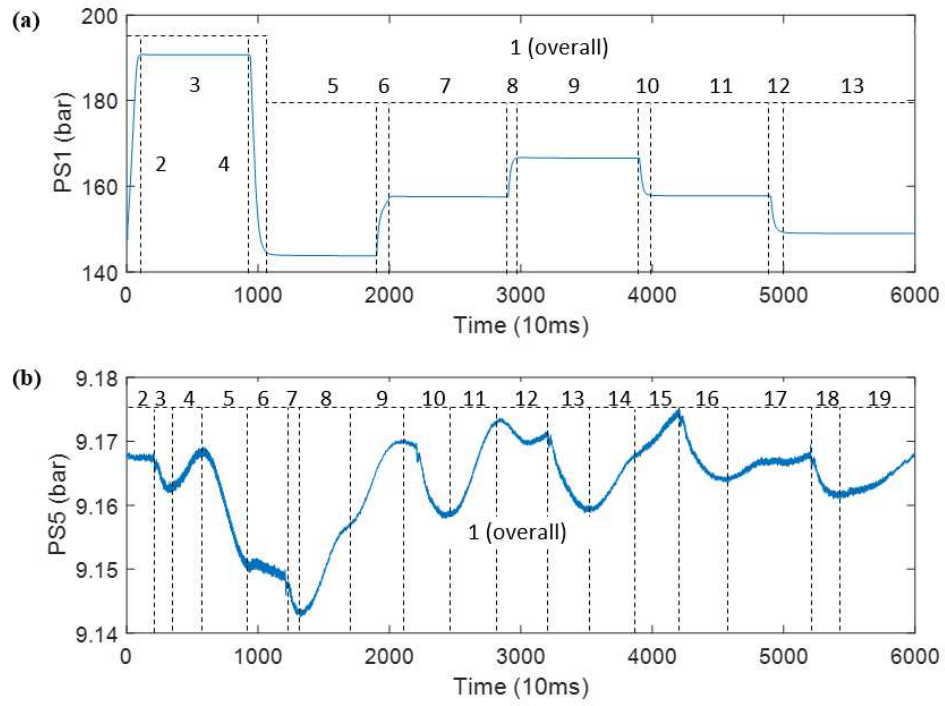
859  
860

**Fig. 1** Systematic diagram of the proposed hybrid novel technique



861  
862

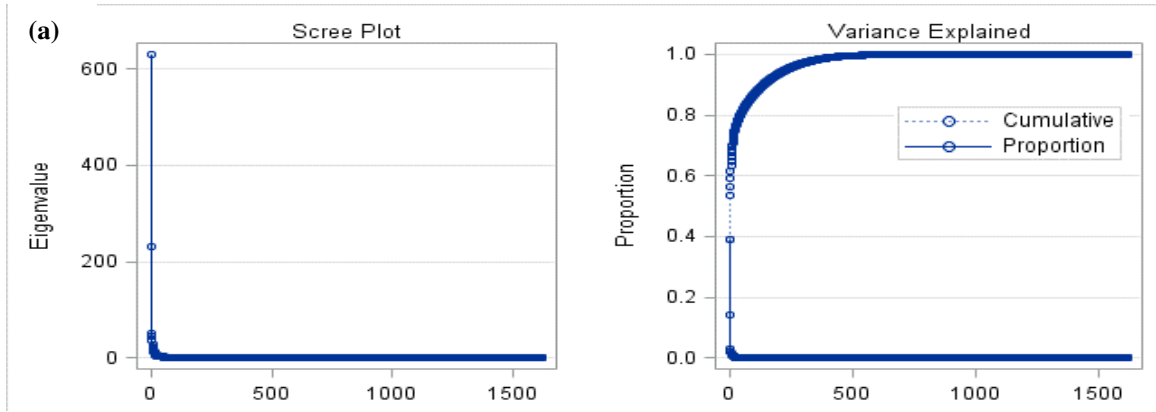
**Fig. 2** Systematic diagram of data pre-processing



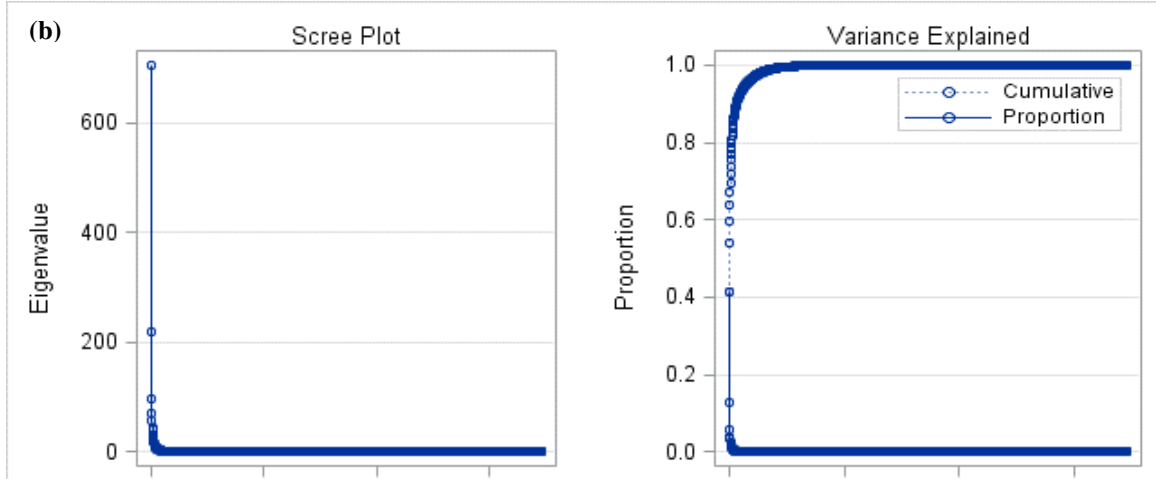
863

864 **Fig. 3** Partition of (a) PS1 and (b) PS5 sensor data into time-intervals

865



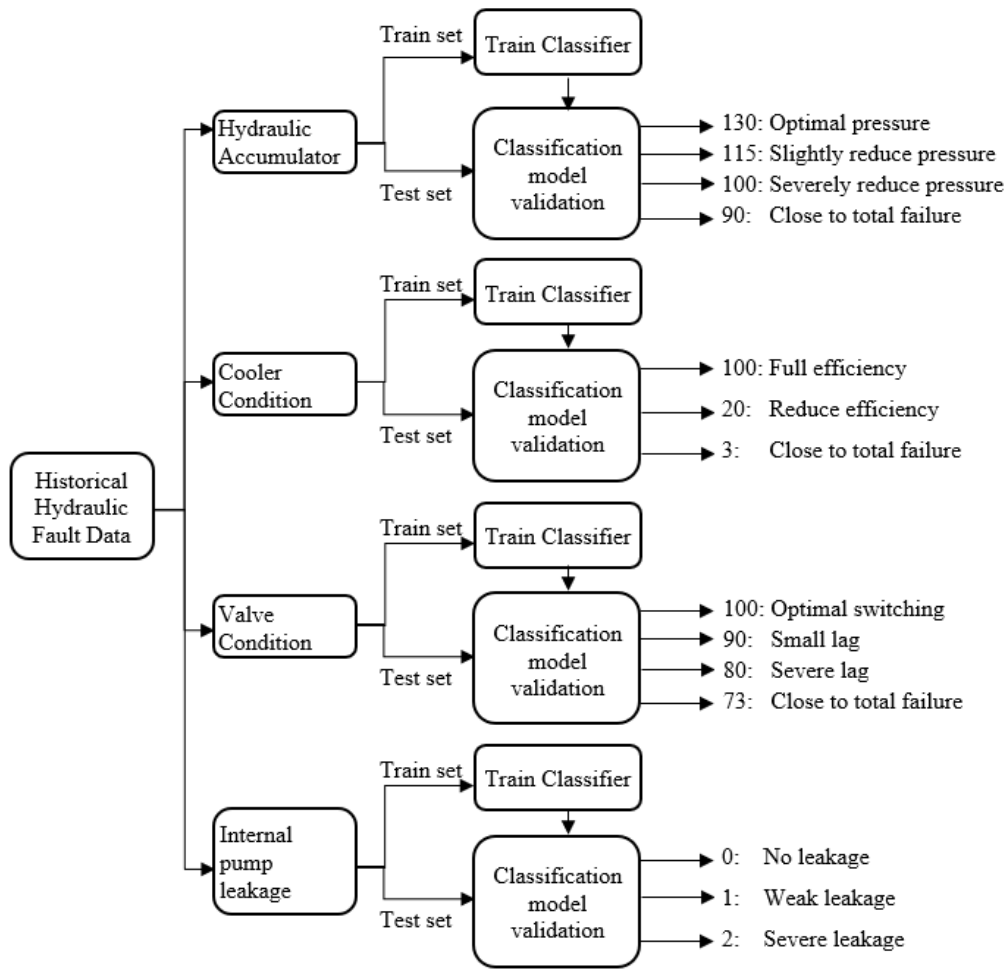
866



867

868

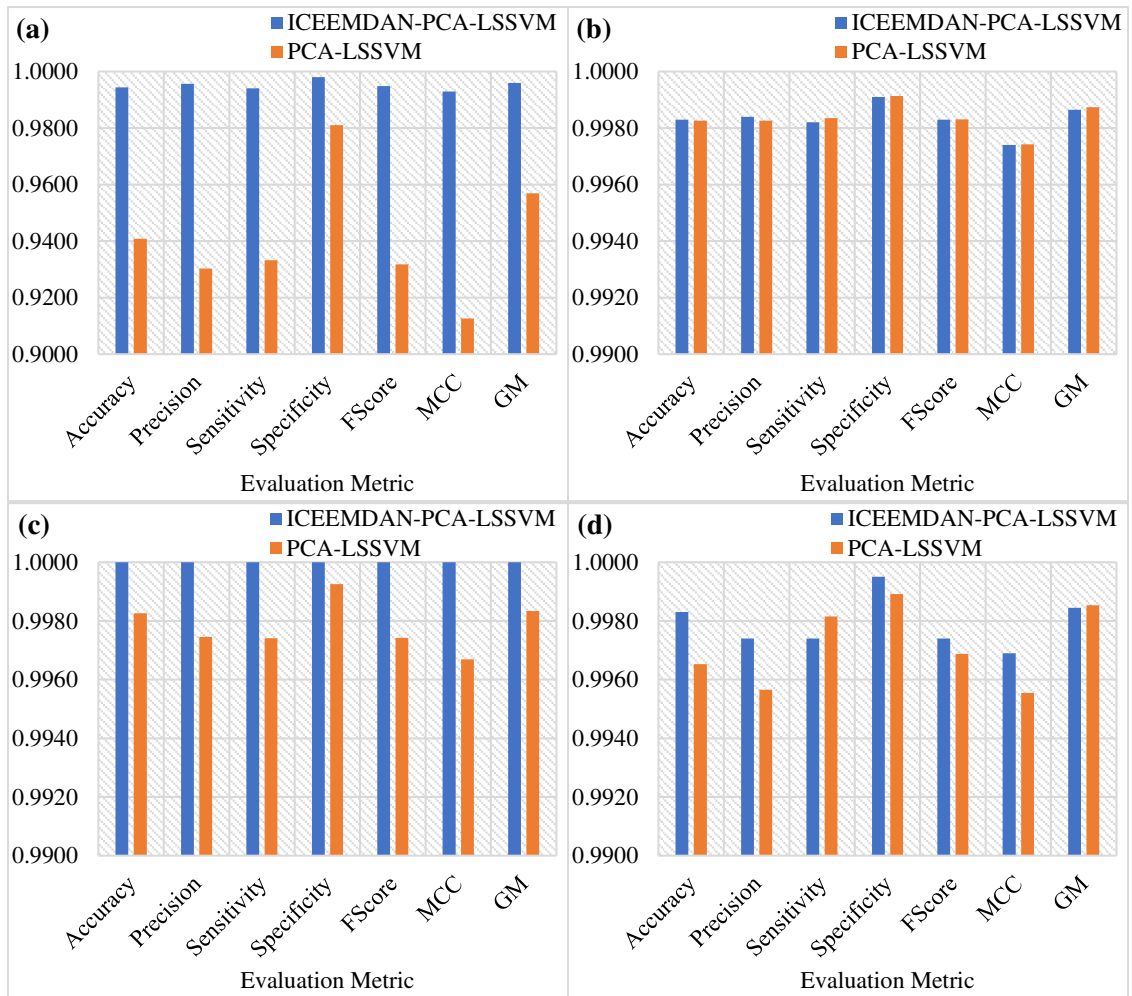
**Fig. 4** Scree plot and variance explained for (a) pre-processed without ICEEMDAN (b) pre-processed with ICEEMDAN



869  
870

**Fig. 5** Multiclass classification procedure

871

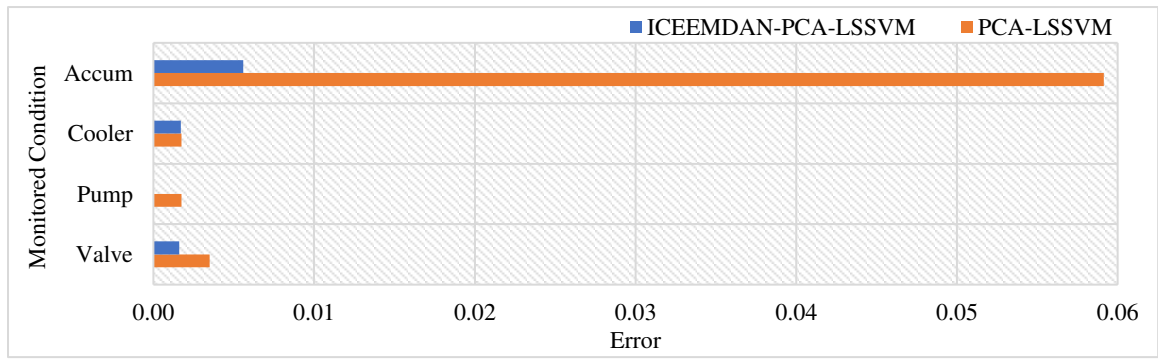


872

873

874

**Fig. 6** Classification performance of ICEEMDAN-PCA-LSSVM and PCA-LSSVM (without ICEEMDAN) for (a) accumulator, (b) cooler, (c) internal pump leakage, and (d) valve conditions



875

876 **Fig. 7** Misclassification rate (error) of ICEEMDAN-PCA-LSSVM and PCA-LSSVM (without ICEEMDAN)

**Table 1** Summary of related works

Year	Objectives	ML Technique Used			Key Findings	Reference
		Pre-processing		Classifier		
		Extraction	Selection			
2015	<ul style="list-style-type: none"> <li>Use scatter-based ML with automated feature extraction and selection capability to develop an adaptive approach for fault classification</li> </ul>	<ul style="list-style-type: none"> <li>Signal shape feature functions (shape slope of linear fit, position of maximum value)</li> <li>Distribution feature functions (median, variance, skewness, kurtosis)</li> </ul>	<ul style="list-style-type: none"> <li>Pearson correlation analysis</li> </ul>	<ul style="list-style-type: none"> <li>LDA</li> <li>ANN</li> <li>SVM (with RBF and linear kernel)</li> </ul>	<ul style="list-style-type: none"> <li>developed an automated feature extraction and selection technique for relevant fault features</li> <li>developed a flexible condition monitoring</li> <li>system for the classification accumulator, cooler pump and valve conditions.</li> </ul>	(Helwig et al. 2015a)
2015	<ul style="list-style-type: none"> <li>Extend prior work of Helwig et al. (2015) in fault diagnosis and the detection of sensor malfunction</li> </ul>	<ul style="list-style-type: none"> <li>Signal shape feature functions (shape slope of linear fit, position of maximum value)</li> <li>Distribution feature functions (median, variance, skewness, kurtosis)</li> </ul>	<ul style="list-style-type: none"> <li>Pearson correlation analysis</li> <li>LDA</li> </ul>	<ul style="list-style-type: none"> <li>KNN</li> </ul>	<ul style="list-style-type: none"> <li>The proposed approach is versatile and capable of detecting sensor malfunctions.</li> <li>Compensates the failure of up to 5 sensors with negligible information loss and reduction in the classification result</li> </ul>	(Helwig et al. 2015b)
2017	<ul style="list-style-type: none"> <li>Automate the reduction in dimension by applying four complimentary feature extraction methods and three features selection algorithms</li> </ul>	<ul style="list-style-type: none"> <li>ALA</li> <li>PCA</li> <li>BFC</li> <li>BDW</li> </ul>	<ul style="list-style-type: none"> <li>Pearson correlation analysis</li> <li>RFESVM</li> <li>Univariate RELIEF</li> </ul>	<ul style="list-style-type: none"> <li>LDA</li> </ul>	<ul style="list-style-type: none"> <li>Reduced the manual effort in feature extraction.</li> <li>The classification of accumulator condition was improved while the others were comparatively similar to the results obtained by Helwig et al. (2015)</li> </ul>	(Schneider et al. 2017)
2019	<ul style="list-style-type: none"> <li>Sought to improve the classification accuracy of prior work.</li> <li>Investigate a trade-off between the number of features and accuracy</li> </ul>	<ul style="list-style-type: none"> <li>Distribution feature functions (mean, variance, skewness, kurtosis)</li> </ul>	<ul style="list-style-type: none"> <li>None</li> <li>OneR</li> <li>J48</li> <li>Information gain</li> </ul>	<ul style="list-style-type: none"> <li>ZeroR</li> <li>OneR</li> <li>JRip</li> <li>PART</li> <li>J48</li> <li>RF</li> <li>NB</li> </ul>	<ul style="list-style-type: none"> <li>Higher accuracy is achieved with the proposed method than prior work.</li> <li>Higher accuracy is still achieved with a lesser number of features</li> </ul>	(Chawathe 2019)
2020	<ul style="list-style-type: none"> <li>Develop a predictive model for the degradation of major components of the hydraulic system</li> </ul>	<ul style="list-style-type: none"> <li>Signal shape feature functions (shape slope of linear fit, position of maximum value)</li> <li>Distribution feature functions (median, variance, skewness, kurtosis)</li> </ul>	<ul style="list-style-type: none"> <li>Pearson correlation analysis</li> <li>LDA</li> </ul>	<ul style="list-style-type: none"> <li>ANN</li> <li>SVM</li> <li>LR</li> <li>DF</li> </ul>	<ul style="list-style-type: none"> <li>High accuracy is achieved when reduction in features allows for optimal combination of inputs that linearly separates the groups while minimising inter-group distance.</li> <li>Selecting features that are highly correlated with target outputs enhances performance</li> </ul>	(Quatrini et al. 2020)
2020	<ul style="list-style-type: none"> <li>Predict different levels of degradation of major components of the hydraulic system</li> </ul>	<ul style="list-style-type: none"> <li>Encodings of the convolution layers</li> </ul>	<ul style="list-style-type: none"> <li>Encodings of the convolution layers</li> </ul>	<ul style="list-style-type: none"> <li>CNN</li> </ul>	<ul style="list-style-type: none"> <li>developed a deep learning-based condition monitoring system for the hydraulic system dataset without explicitly engineering the features</li> </ul>	(König and Helmi 2020)

878

*NB: Classifiers abbreviations are as follows: Linear Discriminant Analysis (LDA), Artificial Neural*

879

*Networks (ANN), Support Vector Machines (SVM), Radial Basis Function (RBF), Logistic Regression (LR),*

880

*Decision Forest (DF), Random Forest (RF), Naïve Bayes (NB), Convolutional Neural Networks (CNN), K*

881 *Nearest Neighbour (KNN), Adaptive Linear Approximation (ALA), Principal Component Analysis (PCA),*  
882 *Best Fourier Coefficients (BFC), Best Daubechies Wavelets (BDW), Recursive Feature Elimination*  
883 *Support Vector Machines (RFESVM)*  
884

885

**Table 2** Details of hydraulic system dataset

Type	Physical Quantity	Sensor	Unit	Sampling Rate (Hz)	Class	Time Interval
Sensor	Pressure	PS1	bar	100	Regression	13
		PS2				14
		PS3				18
		PS4				25
		PS5				19
		PS6				19
	Motor Power	EPS1	W	10		13
	Volume Flow	FS1	l/min			18
		FS2		18		
	Temperature	TS1	°C	1		7
		TS2				7
		TS3				8
		TS4				15
	Vibration	VS1	mm/s	15		
Cooling Efficiency	CE	%	13			
Cooling Power	CP	kW	13			
System Efficiency	SE	%	23			
Hydraulic Component	Accumulator	-	bar	-	Classification	
	Cooler		%			
	Internal Pump Leakage		-			
	Valve		%			

886

Source: Modified after Helwig et al. (2015)

**Table 3** Summary of PCA results of denoised and undenoised data

Pre-Processed without ICEEMDAN				Pre-Processed with ICEEMDAN			
PC	Eigenvalue	Proportion	Cumulative	PC	Eigenvalue	Proportion	Cumulative
1	630.4540	0.3906	0.3906	1	705.0536	0.4145	0.4145
2	232.4312	0.1440	0.5346	2	220.0692	0.1294	0.5439
3	50.9179	0.0315	0.5662	3	95.9180	0.0564	0.6003
4	44.5339	0.0276	0.5938	4	69.1454	0.0406	0.6409
N	N	N	N	N	N	N	N
160	1.0071	0.0006	0.9150	81	1.0160	0.0006	0.9598
161	1.0024	0.0006	0.9156	82	1.0067	0.0006	0.9604
162	0.9791	0.0006	0.9162	83	0.9963	0.0006	0.9609
N	N	N	N	N	N	N	N

889

**Table 4** Multiclass classification of fault conditions based on ICEEMDAN-PCA-LSSVM

Hydraulic Component	Training		Testing		
	Accuracy $\pm$ STD	CPU Time (sec)	Accuracy $\pm$ STD	Best	Worst
Accumulator	1.0000 $\pm$ 0.000	38.2344	0.9944 $\pm$ 0.0007	0.9948	0.9930
Cooler	1.0000 $\pm$ 0.000	9.1250	0.9983 $\pm$ 0.0006	1.0000	0.9948
Pump	1.0000 $\pm$ 0.000	32.4375	1.0000 $\pm$ 0.0000	1.0000	1.0000
Valve	1.0000 $\pm$ 0.000	22.1094	0.9984 $\pm$ 0.0005	1.0000	0.9983

890

891

**Table 5** Accumulator condition classification rate

Metric	Pre-Processed with ICEEMDAN-PCA				Pre-Processed PCA (without ICEEMDAN)			
	LSSVM	LDA	SVM	ANN	LSSVM	LDA	SVM	ANN
Accuracy	0.9944	0.9896	0.9913	0.9791	0.9409	0.9270	0.8904	0.8591
Error	0.0056	0.0104	0.0087	0.0209	0.0591	0.0730	0.1096	0.1409
Precision	0.9956	0.9880	0.9913	0.9772	0.9303	0.9185	0.8762	0.8494
Sensitivity	0.9941	0.9871	0.9901	0.9778	0.9333	0.9239	0.8798	0.8400
Specificity	0.9980	0.9966	0.9971	0.9931	0.9810	0.9766	0.9644	0.9527
F Score	0.9948	0.9874	0.9906	0.9775	0.9317	0.9192	0.8772	0.8438
MCC	0.9929	0.9842	0.9878	0.9705	0.9126	0.8970	0.8420	0.7977
GM	0.9960	0.9918	0.9936	0.9854	0.9569	0.9499	0.9212	0.8945

892

**Table 6** Cooler condition classification rate

Metric	Pre-Processed with ICEEMDAN-PCA				Pre-Processed PCA (without ICEEMDAN)			
	LSSVM	LDA	SVM	ANN	LSSVM	LDA	SVM	ANN
Accuracy	0.9983	0.9948	0.9948	0.9983	0.9983	0.9948	0.9965	0.9965
Error	0.0017	0.0052	0.0052	0.0017	0.0017	0.0052	0.0035	0.0035
Precision	0.9984	0.9949	0.9949	0.9983	0.9983	0.9950	0.9964	0.9966
Sensitivity	0.9982	0.9949	0.9949	0.9983	0.9983	0.9948	0.9966	0.9966
Specificity	0.9991	0.9974	0.9974	0.9991	0.9991	0.9973	0.9983	0.9982
F Score	0.9983	0.9949	0.9949	0.9983	0.9983	0.9949	0.9965	0.9966
MCC	0.9974	0.9922	0.9922	0.9974	0.9974	0.9922	0.9948	0.9948
GM	0.9986	0.9961	0.9961	0.9987	0.9987	0.9961	0.9974	0.9974

**Table 7** Internal pump leakage condition classification rate

Metric	Pre-Processed with ICEEMDAN-PCA				Pre-Processed PCA (without ICEEMDAN)			
	LSSVM	LDA	SVM	ANN	LSSVM	LDA	SVM	ANN
Accuracy	1.0000	0.9861	1.0000	0.9704	0.9983	0.9948	0.9878	0.9165
Error	0.0000	0.0139	0.0000	0.0296	0.0017	0.0052	0.0122	0.0835
Precision	1.0000	0.9807	1.0000	0.9597	0.9975	0.9924	0.9825	0.8832
Sensitivity	1.0000	0.9793	1.0000	0.9623	0.9974	0.9953	0.9819	0.8841
Specificity	1.0000	0.9940	1.0000	0.9862	0.9993	0.9978	0.9948	0.9619
F Score	1.0000	0.9794	1.0000	0.9610	0.9974	0.9938	0.9820	0.8836
MCC	1.0000	0.9739	1.0000	0.9467	0.9967	0.9911	0.9769	0.8453
GM	1.0000	0.9866	1.0000	0.9742	0.9983	0.9965	0.9883	0.9222

**Table 8** Valve condition classification rate

Metric	Pre-Processed with ICEEMDAN-PCA				Pre-Processed PCA (without ICEEMDAN)			
	LSSVM	LDA	SVM	ANN	LSSVM	LDA	SVM	ANN
Accuracy	0.9984	0.9983	0.9965	0.9548	0.9965	0.9948	0.9930	0.8783
Error	0.0016	0.0017	0.0035	0.0452	0.0035	0.0052	0.0070	0.1217
Precision	0.9976	0.9974	0.9948	0.9451	0.9957	0.9924	0.9921	0.8536
Sensitivity	0.9977	0.9974	0.9948	0.9469	0.9982	0.9953	0.9929	0.8649
Specificity	0.9995	0.9995	0.9990	0.9843	0.9989	0.9978	0.9976	0.9584
F Score	0.9976	0.9974	0.9948	0.9457	0.9969	0.9938	0.9925	0.8585
MCC	0.9972	0.9969	0.9938	0.9300	0.9955	0.9911	0.9899	0.8160
GM	0.9986	0.9985	0.9969	0.9654	0.9985	0.9965	0.9952	0.9105